Compensation Topologies in IPT Systems: Standards, Requirements, Classification, Analysis, Comparison and Application

VIKTOR SHEVCHENKO[1], **(Student Member, IEEE),**
OLEKSANDR HUSEV[1,3], **(Senior Member, IEEE),**
RYSZARD STRZELECKI[2,4], **(Senior Member, IEEE),**
BOHDAN PAKHALIUK[1,2], **(Student Member, IEEE),**
NIKOLAI POLIAKOV[4], **AND NATALIA STRZELECKA**[5]

[1]Chernihiv Power Electronics Laboratory, Chernihiv National University of Technology, 14000 Chernihiv, Ukraine
[2]Faculty of Electrical and Control Engineering, Gdansk University of Technology, 80-233 Gdansk, Poland
[3]Power Electronics Research Group, Tallinn University of Technology, 12616 Tallinn, Estonia
[4]Faculty of Control Systems and Robotics, ITMO University, 197101 Saint Petersburg, Russia
[5]Faculty of Electrical Engineering, Gdynia Maritime University, 81-225 Gdynia, Poland

Corresponding author: Viktor Shevchenko (shevaip@gmail.com)

ABSTRACT Wireless power transfer devices are becoming more relevant and widespread. Therefore, an article is devoted to a review, analysis and comparison of compensation topologies for an inductive power transfer. A new classification of topologies is developed. A lot of attention is paid to the problems of the physical fundamentals of compensation work, standards, safety, and five main topology requirements. It is determined, that topologies with the series primary compensating are the most effective in the IPT for charging devices among the four classical schemes. The series-parallel solution is recommended in case of the low output voltage, minimum size of a secondary side coil is achievable. The series-series solution does not depend on the magnetic coupling coefficient and the load on the resonance frequency. For the convenience of displaying and understanding the information, the comparison results are listed in the tables, graphs and dependencies. The main suitable topologies for a certain application are defined. The given conclusions provide a "one-stop" information source and a selection guide on the application of compensation topologies both in terms of devices and in terms of power level that is the main value of this paper. During literature analysis and recent trends in the market for wireless power transmission devices, the main possible further ways of developing topologies are underlined. First of all, it concerns increasing the frequency of resonance of compensation topologies, the use of multilevel / multi-pulse / multicoils structures, the study of existing high-frequency semiconductors and the development of the semiconductor and magnetic materials.

INDEX TERMS Wireless power transfer, inductive power transfer, compensation topology, requirement, classification, standards, application.

NOMENCLATURE

A4WP	= Alliance For Wireless Power;
ARIB	= Association of Radio Industries and Businesses;
BWF	= Broadband Wireless Forum;
CC	= Constant Current;
CCSA	= China Communication Standard Association;
CISPR	= International Special Committee on Radiofrequency Interference;
CPT	= Capacitive Power Transfer;
CV	= Constant Voltage;
EMF	= Electromagnetic Field;
Ers	= Energy-Harvesting Receivers;
EV	= Electric Vehicle;
EVES	= Eavesdroppers;

GSM = Global System For Mobile Communications;
ICNIRP = International Commission On Non-Ionizing Radiation Protection;
IEC = International Electrotechnical Commission;
IEEE = Institute Of Electrical And Electronics Engineers;

IPT = Inductive Power Transfer;
ISM = Industrial Scientific And Medical Frequency Band;
ISO = International Organization for Standardization;
ITU-R = International Telecommunication Union – Radiocommunication;
LIO = Load-Independence Output;
LED = Light-Emitting Diode;
LCL = Inductance-Capacitance-Inductance;
LCC = Inductance-Capacitance-Capacitance;
MIMO = Multiple-Input Multiple –Output;
MISO = Multiple-Input Single-Output;
MIT = Massachusetts Institute Of Technology;
MPPT = Maximum Power Point Tracking;
OLEV = On-Line Electric Vehicle;
PP = Parallel-Parallel Compensation;
PS = Parallel-Series Compensation;
Qi = Standard Of Wireless Power Consortium;
RF = Radio Frequency;
RFID = Radio Frequency Identification;
RMS = Root Mean Square;
SAE = Society Of Automotive Engineers;
SIMO = Singe-Input Multiple -Output;
SISO = Singe-Input Single-Output;
SP = Series-Parallel Compensation;
SS = Series-Series Compensation;
TTA = Telecommunication Technology Association;
V2G = Vehicle-To-Grid System;
VA-Rating = Volt Ampere Characteristics;
VSI = Voltage Source Inverter;
WBAN = Wireless Body Area Networks;
WPT = Wireless Power Transfer;
ZCS = Zero Current Switch;
ZPA = Zero Phase Angle;
ZVS = Zero Voltage Switch.

I. INTRODUCTION

The investigations in the field of green energy and an electric transport are supported by the governments in many countries and are a strategy for the future development and technology. Accordingly, the wireless communication methods for a power transfer and transmitting information between the devices that have well-known advantages over connectors are also actively developing.

Among the various methods of Wireless Power Transfer (WPT), the most practical use is the capacitive and inductive methods. In the first case, the transmitter and the energy receiver are the plates of the air capacitor (Fig. 1a), in the other case are the air-gap transformer coil (Fig.1b). The most significant advantage of the Capacitive Power Transfer (CPT) over the Inductive Power Transfer (IPT) [1] at lower power levels is its cost and size. The capacitive method has a greater transmission distance especially on a low-power level, rather than in the method of electromagnetic induction, but lower efficiency and the transmission power [1]–[3].
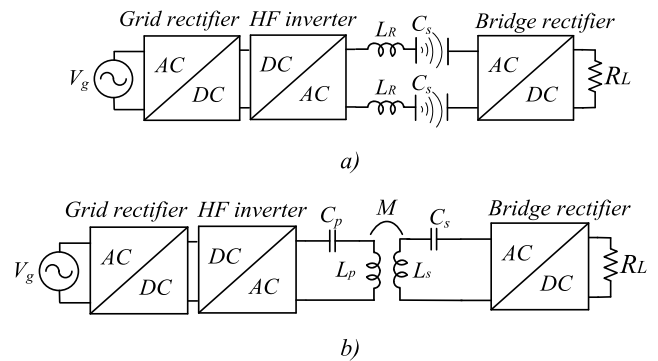

FIGURE 1. Typical schemes of WPT: a) CPT technology; b) IPT technology.

The advantages of the magnetic inductive coupling include also the ease of implementation, convenient operation, high efficiency on a close distance (typically less than a coil diameter, but can be increased in a resonance system) and ensured safety [4]. Therefore, mass commercial and industrial distribution especially in the high-power applications has been received by an inductive method and an inductive method with resonance as its type.

The energy from the grid through the primary rectifier enters the high-frequency inverter where it is converted into the alternating current. Through a primary resonant circuit C_p-L_p with magnetically coupled coils the energy is transmitted from the primary side to the side of the device (secondary side). The resulting current is rectified, filtered and fed to the load (R_L).

In the WPT by electromagnetic induction, a near-field Electromagnetic Field (EMF) is used. It is known that due to the electrodynamic induction, the alternating high-frequency electric current flowing through the primary winding creates an alternating magnetic field (Ampre's law) that acts on the secondary winding, inducing it in the electric current (Faraday's law) [5] – Fig.2. To achieve high efficiency, the interaction must be sufficiently close. When the secondary winding is removed from the primary, most of the magnetic field does not reach the secondary winding and the inductive coupling becomes increasingly ineffective due to the losses.

Systems with only inductive coupling have a much lower efficiency than IPT with the resonance. The large air gap of the transformer increases the leakage of the flow and, as a result, leads to a higher leakage inductance compared to the conventional transformers. The efficiency of IPT without compensation as a rule does not exceed 50% [6].
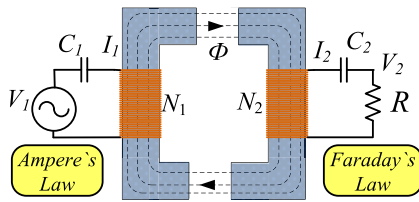
FIGURE 2. Basic principle of IPT [7].

To compensate the leakage inductance, the reactive power on the primary and secondary sides additional compensating capacitors are required (Fig.2) [6]–[8]. In this case, the possible distance between the coils increases and thus the efficiency of the transferred power decreases less slowly [9]. Further in this article under the IPT will be understood the IPT with compensation circuits (inductive power transfer system with resonance).

The conductors are wound on the magnetic conductive material to direct the flow and improve the coupling coefficient and efficiency. In Fig.3: N_1, N_2 are the numbers of turns on the primary and secondary sides respectively; I_1, V_1, I_2, V_2 -current and voltage on the primary and secondary sides; C_1, C_2-compensating resonant capacitors; R - load resistance, Φ -magnetic flux.
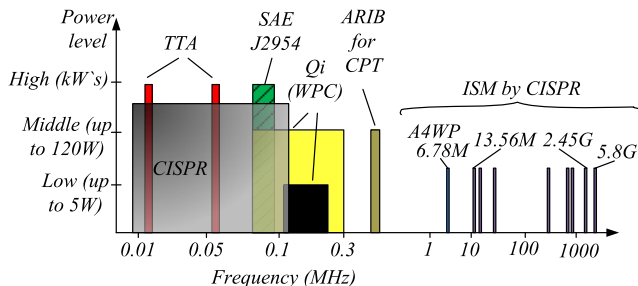

FIGURE 3. Frequency standards and power levels.

The use of compensation topologies also increases the transfer power, reduces the Volt-Ampere rating (VA rating) of the power source and helps to achieve a soft switching of semiconductors [10], [11].

A. FREQUENCY STANDARTS AND SAFETY

The resonant frequency is selected based on the load and can vary in a wide range. In the case of using the topology of compensation in the IPT, the energy is transmitted with a certain resonance frequency, hence the quality factor of the system is higher, but the exact adjustment of the resonant frequencies is required. The primary and secondary sides can be tuned to approximately the same resonant frequency. This allows to cancel the secondary leakage inductance and to maximize the power transfer efficiency.

For a particular group of applications, researchers use the same frequencies. There are ranges and frequency groups that are standardized. This section describes the most important global standards and frequencies.

The operating frequency for light duty electric vehicle wireless charging is 81…90.00 kHz, which is regulated by the Society of Automotive Engineers (SAE) Task Force's J2954 standard. It is recommended to set 85 kHz for Electric Vehicle (EV) applications [12], [13].

For heavy duty vehicle the standard SAE J2954 is also relevant, which corresponds to International Telecommunication Union -Radiocommunication (ITU-R) [14].

Operating frequency for portable and mobile devices is regulated by Qi standard of Wireless Power Consortium [15]. Low-power category can transfer the power within 5 W on 110 to 205 kHz frequency range and a medium-power category can deliver the power up to 120 W on 80-300 kHz frequency range (Fig.3) [16].

When the size of the devices is compact with a power of several watts, as well as for medical applications, mainly is used the megahertz range - Industrial Scientific and Medical high-frequency applications (ISM) frequency band, which belongs the International Special Committee on Radiofrequency Interference (CISPR). The allowed frequency band is discrete (Fig.3) [17], [18]. For example, the available frequency range of 6.78 MHz is 15 kHz and 13.56 MHz is 7 kHz [17]. The frequency range from 9 to 135 kHz is used less commonly. Range below 135 kHz is mainly used by radio services [17], household appliances, ignition systems, and fluorescent lamps [19].

Standard Alliance for Wireless Power (A4WP) aims to provide the spatial freedom for the wireless power [20]. This standard proposes to generate a larger electromagnetic field with a resonance coupling. To achieve spatial freedom, the A4WP standard does not require a precise alignment and even allows a separation between a charger and charging devices. The maximum charging distance is up to several meters, working at 6.78 MHz. This is the frequency used for a power transfer. The A4WP standard uses the 2.4 GHz ISM band. It is divided into five categories with the output power up to 6.5 Watts. Moreover, multiple devices can be charged concurrently with a different power requirement, for example a laptop, tablet and smartphone. Another advantage of A4WP over Qi is that foreign objects can be placed on an operating A4WP charger without causing any adverse effect [4].

There is a standard International Electrotechnical Commission (IEC) with two power groups: up to 5 watts and up to 15 watts, which includes multi-device WPT support. The IEC and SAE J2954 synchronized with International Organization for Standardization (ISO) [19].

There are several local standards and frequency ranges in China, Japan and Korea [19]. They are classified by frequency bands for certain groups of devices and power. It is an inductive coupling: low power; inductive coupling: high power (several watts up to 1.5 kW); magnetically coupling resonant (up to 100W), capacitive coupling.

The China has its own standard - China Communication Standard Association (CCSA). Japan has the Association of Radio Industries and Businesses (ARIB); Broadband Wireless Forum (BWF) for power up to 7.7 kW. In the

CPT transmitted up to 100W power on the frequency 425 kHz–524 kHz, provided by ARIB [19].

There is Telecommunication Technology Association (TTA) In Korea. For buses and trains, industrial vehicles, with stationary and dynamic charging with a power of tens or more kilowatts (up to 100 kW), frequencies of 19-21 kHz and to 59-61 kHz are usually used. These are such systems as: On-Line Electric Vehicle (OLEV) [21], EATON, IPT Technology, WAVE and others [22].

Users are interested in the impact of electromagnetic radiation from WPT devices on a human health. In [23] is discussed a biological response caused by the exposure to electric and magnetic fields from 1 Hz to 100 kHz, heating in human tissue, surface electric discharge, induction in the retina of phosphenes, heating in implanted medical devices and metals.

Devices with a centimeter scale are not suitable for some critical application, e.g., cardiac implants. There is a trade-off between the implant size and the WPT efficiency. The optimal frequency for WPT in implanted devices lies in the sub-GHz to low-GHz range [24].

International Commission on Non-Ionizing Radiation Protection (ICNIRP) has set the internal electric field limit $1.35 \times 10^{-4} f$, where f is a frequency of the electric field and the typical limit is 83V/m. The magnetic field for human tissues equals $27\mu T$ (21.4A/m) for a magnetic field [7], [12], [23]. The leakage EMF must comply also with more rigid IEEE C95.1-2345 Standard [25], which offers more insights into physiological effects such as nerve excitation on less 100 kHz and the tissue heating above 100 kHz. In order to protect the driver and passengers in electric vehicles, metal protective screens can be installed [7], [21].

B. REQUIREMENTS FOR COMPENSATION

The basic requirements for compensation schemes are described in [7], [10]. The list of requirements and what they depend on is shown in Table 1.

TABLE 1. Requirements for compensation network.

Requirement	Realization (Depends on)
Minimized VA rating and maximized power transfer	Leakage inductance, compensation topology
CC or CV output	Application, compensation topology
High efficiency	Coupling coefficient, quality factors of the windings, soft switching
Bifurcation resistant	Load quality factor, compensation topology and capacitor
High misalignment tolerant	Compensation topology

One of the requirements is to minimize the volt-ampere characteristics of the source and increase transmission power. These requirements can be achieved by reducing the leakage inductance [7]. The primary resonance cancels the primary

leakage inductance, thereby increasing the power factor to near unity, with the secondary coil also operating at or near the same resonant frequency [26]. A separate direction is the Maximum Power Point Tracking (MPPT) and the maintenance of the system at this point or at a certain area of the power curve.

The advantage for certain systems, such as wireless charging, power Light-Emitting Diodes (LEDs), etc. will provide a constant voltage or current output mode. Also, in Constant Current (CC) or Constant Voltage (CV) modes should be high efficiency of the energy transfer. It depends on the coupling coefficient and the quality factor of the inductances, as well as on the resonant frequency of the secondary and primary sides. When changing the position of the coils, this leads to the need to change the frequency of operation. The sensitivity to changing position (misalignment) in each topology of compensation is different. This requires a more complex control algorithm so that on both sides the resonance frequency remains the same. High efficiency can be achieved by soft switching of semiconductors [10].

Inverters may operate with a constant or variable frequency depending on the control strategy and soft commutation requirements. Those operating with variable frequency are subjected to a phenomenon known as Bifurcation, which is the occurrence of multiple zero phase angle resonant frequencies that can lead the converter to unstable operating modes [27]. This phenomenon is caused by the input impedance (Z_i) that may vary roughly from capacitive to inductive depending on secondary quality factor (Q_s) and this may cause unstable operating modes [28] (Fig.4).
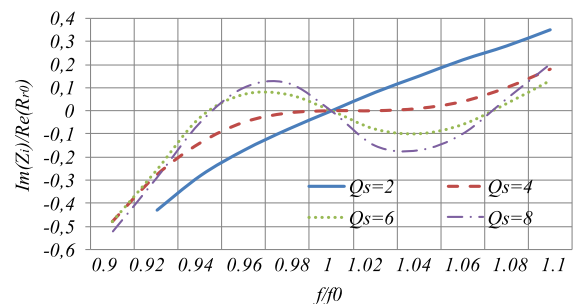

FIGURE 4. Example of bifurcation occurrence in SS topology [27].

Therefore, the compensation network must be designed for a single zero phase angle, and ensure the system stability for a variable frequency control under different loading conditions [7], [10]. For operating without the bifurcation, the frequency controller must be designed to operate within the bifurcation. If the system can work in the bifurcation area, the controller must anticipate and correctly work in the desired mode of the operation.

The latest requirement for the bifurcation criterion in combination with the frequency and load controller ensures the stable and high performance of the WPT system. That is, the more requirements are met, the more efficient the IPT scheme will be with compensation.

II. CLASSIFICATION OF COMPENSATION TOPOLOGIES

The compensation for an inductive energy transfer can be considered as a topology in which there is at least one resonant element on one side. Figure 5 depicts the proposed classification of the topology compensation.
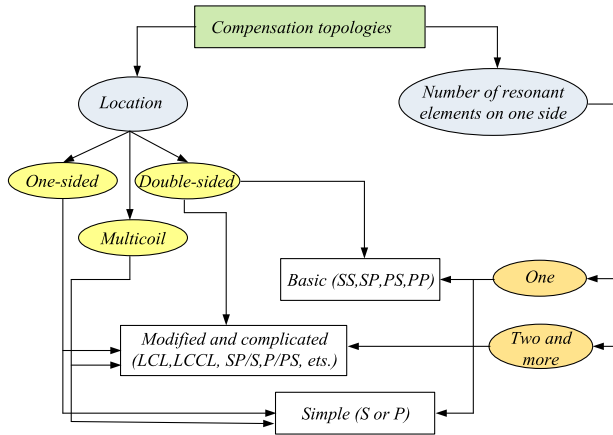

FIGURE 5. Classification of compensation topologies.

The topologies are proposed to be classified according to the location (on the primary or secondary side, double-sided and multicoils, if there are several transmitting or receiving coils). Resonant elements on either side may be one, two or more. These may be capacitors and inductors. In the case of multicoils, the compensating element or elements can be located near each coil, only on the transmitter or on the receiving side, or on both.

The classical (or basic) topologies of compensation are the topologies that have one compensating capacitor on both sides. They are discussed in more detail in the next section. On their basis different combinations of topologies have been developed, and are considered in section V.

In the case of another type compensation topologies or their combinations, the complexity of a parameter calculation and the prediction of the system behavior increases, from the increase in the number of elements the reliability decreases. The number of compensating capacitors can be two or more, there may also be an additional inductance. Other topologies have certain advantages, so they can be used. These questions are described in section V. Also, the disadvantages can be called the greater complexity and cost of such systems, especially with the adding of additional inductances.

III. REVIEW AND ANALYSIS OF 4 BASIC COMPENSATION TOPOLOGIES

There are 4 basic compensating topologies (Fig. 6), based on which most semiconductor solutions are created: Serial-Serial (SS), Serial-Parallel (SP), Parallel-Serial (PS) And Parallel-Parallel (PP).

The investigation of WPT was conducted long time ago, but since the 90s, more attention has been paid to IPT systems with the compensation [29].
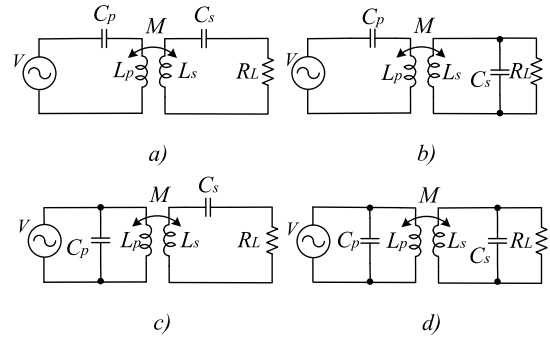

FIGURE 6. Classification of basic compensation topologies:
a) Series-Series (SS); b) Series-Parallel (SP); c) Parallel-Series (PS);
d) Parallel-Parallel (PP).

At that time, the markets of electric cars and mobile phones began. Initially, the formulas for determining the primary compensating capacity were different, without taking into account certain parameters and specifics of the process. Some designs calculate the primary capacitance by compensating only the primary self-inductance [30]. This is acceptable if the reflected impedance is negligible in comparison to the primary self-inductance. Moreover, the bifurcation-free operation is normally assumed.

Initially, mainly purely inductive methods of WPT for charging electric cars were considered [31]–[36].

But a real impetus to the development of WPT with compensation was a well-known study in Massachusetts Institute Of Technology (MIT) in 2007 [37]. The research team in MIT found that when the transmission coils work under the resonance, the efficiency and the transfer distance can be improved [38].

A. ANALYSIS OF BASIC TOPOLOGIES

In order to understand the features of the basic compensation topologies, they need to be considered in detail. The basic equations and the results of the comparison are listed in the Tables 2-6.

A detailed analysis of the basic compensation topologies is presented in [7], [8], [10], [39]–[41]. In [42] it is determined that the choice of the L and C values of the resonant circle depends mainly on the primary or secondary topology, the quality factor and the value of the magnetic coupling coefficient. Comparing the SS with the SP parameters, it can be seen that the choice of a topology strongly influences the choice of a primary capacity.

The choice of the primary compensation topology also depends on the application [43]. A series compensation is well suited for systems with long primary tracks, with the compensation capacitors placed in series along the track. This allows the track voltages to be managed within the maximum allowable limits. The parallel compensation is better suited for concentrated windings, as these are usually high current systems. A single capacitor at the terminals of the coil is used.

TABLE 2. Primary capacitance Cp for basics topologies [28], [40].

Topo-logy	Equation	№ of formula
SS	$C_p = \dfrac{1}{\omega_r^2 \cdot L_p}$	1
SP	$C_p = \dfrac{1}{\left(L_p - \dfrac{M^2}{L_s}\right)\cdot \omega_r^2}$	2
PS	$C_p = \dfrac{L_p}{\left(\dfrac{\omega_r^2 \cdot M^2}{R}\right)^2 + \omega_r^2 \cdot L_p^2}$	3
PP	$C_p = \dfrac{L_p - M^2/L_s}{\left(\dfrac{M^2 \cdot R}{L_s^2}\right)^2 + \omega_r^2 \cdot \left(L_p - M^2/L_s\right)^2}$	4

Considering the capacitor requirements, the series compensation implies higher voltages and lower currents than the parallel compensation. In the SP topology, the primary-side capacitance affects the power factor and input-to-output voltage ratio of the resonant circuit, which consists of the compensation capacitors and two coils [44]. Therefore, the capacitance of the primary-side capacitor affects the total effciency including the effciencies of the inverter and resonant circuit.

The SS and SP compensation are most often used in the practical applications and implementation, because they have the best efficiency [10], [45] which is further analyzed. Details for the effectiveness and thorough research and comparison of these two topologies under different conditions and changes in various parameters can be found in [45].

In most of the discussed articles, the effectiveness of these two topologies was more than 93%, and in many cases it is approaching 97% at different transmission power [19], [40].

The compensations with a parallel capacitor on the primary side are rarely used [46], [47] due to the large input impedance, the complexity of the calculations, dependence on the coupling coefficient and load, and other disadvantages. Although some sources indicate that the PS compensation scheme provides a soft switching of all semiconductor devices [48]. A topology may be appropriate, for example, for transmitting energy from solar panels at specific input parameters that provide VA ratting of photovoltaic panels [48].

The biggest advantage of the SS topology is the fact that the compensation capacities do not depend neither on the magnetic coupling coefficient $k = M/\sqrt{L_p \cdot L_s}$ nor the load on the resonance frequency (1) [6], [8], [49]. To illustrate the dependence of the compensation on the coupling coefficient, it is necessary to calculate the capacitors for operation at the resonant frequency (Table 2).

On the contrary, the SP topology depends on the coupling factor (2) and requires a greater value of the primary capacity for a strong magnetic coupling [8], [42], [50].

The primary capacitor for SS topology is calculated as (1), only the primary inductor Lp and the resonance frequency ω_r need to be substituted [1], [28], [40]. For SP topology, the primary capacity is determined by (2), where the mutual inductance M means the dependence of the calculated value on the coupling coefficient. The choice of the topology strongly influences the choice of the primary capacity.

For the SS and SP topologies, the secondary compensating capacitor Cs is also calculated from (1) [40], but it is necessary to substitute the value of the secondary inductance *Ls*.

Two other topologies with a parallel primary compensating capacitor PS and PP have considerably more bulky formulas for calculating the primary capacitance (3), (4). In addition, the value of the resonance capacity depends not only on the change in the coupling factor, but also on the change in the load resistance [1], [28].

To improve the efficiency of the PS and PP, the topology requires the additional serial inductance for improved inverter current control (transformation in Inductance-Capacitance-Capacitance (LCC), CCL, etc.) flowing in the parallel resonant circuit [42]. This inductance increases the size of the converter and the cost of the system. Another drawback is that it requires the current source input to avoid any instantaneous change in the voltage [51]. Another important fact is the value of the input resistance, which is especially large in PS and PP topologies [52]. This requires a high driving voltage to transfer the sufficient amount of power.

On the resonance frequency, the voltage gain in PP topology is related to the load and the transformer parameters, and its gain is less than 1 for all loads. The voltage ratio presents a different value for different values of the load [6].

In [28] it is noted, that PP topology has been chosen since it is commonly used for high-power industrial [53]. The current source characteristic of the parallel-compensated secondary is suited for battery charging, whereas the parallel-compensated primary is used to generate a large primary current [43].

The PP topology requires a slightly larger primary capacitance for loose coupling with a low secondary quality factor, but needs a smaller primary capacitance if the coupling is improved or the secondary quality factor is increased. A smaller primary capacitance is always required for PS topology and the change becomes larger with better coupling or higher secondary quality factor [50].

The PP configuration suffers from the low power factor, a high load voltage of the parallel secondary and large current source requirements of the parallel primary [10], [26].

The main advantages of the PS and PP topologies are the high efficiency and high power factor at relatively low mutual inductance and a relatively large range of the load variation and mutual inductance [51], [54]. The acceptable efficiency will be at a rather small value of the coupling coefficient and,

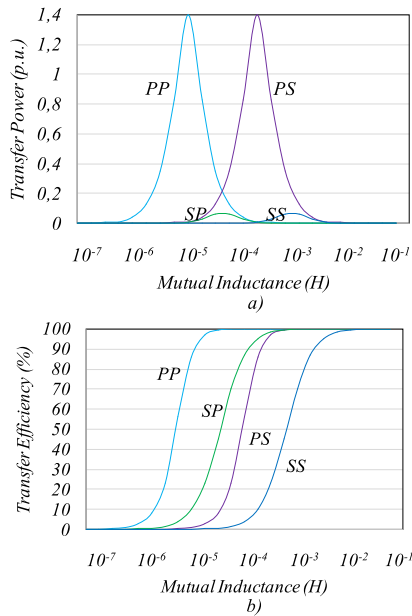consequently, mutual inductance, as defined in the simulation (Fig.7).

FIGURE 7. Comparison of dependences on mutual inductance for basic topologies: a) transfered power; b) efficiency [54].

At low-power levels, where the wire section is not a relevant parameter, PS and PP compensations make it possible working at a slightly larger distance with the same operating frequency [55].

The series compensation requires a higher voltage and current than the parallel compensation [56].The application of the SS compensation is more expedient for a large power with variable load parameters, such as charging electric accumulators with a load of several kilowatts [6], [11], [21], [42], [57]. Also SS compensation is especially useful in segmented dynamic wireless power transfer applications, where the coupling coefficient varies with movement of the EV [7] and the voltage transferred to the secondary is very high.

The analysis of the 200 kW system was carried out in [55]. It is determined that the SS compensation is the one requiring less copper mass. The SP compensation requires 4.6% more, PS 30% more, and the PP compensation 24% more. Although the SS compensation is the option requiring less copper mass, using parallel primary compensation the operating frequency is much lower, being just 11 kHz for the PS compensation. That is due to the fact that the lower the required current (and thus the wire section) is, the higher the operating frequency will be. This implies higher switching frequencies in the topologies using the series primary compensation, although from an economical point of view, the SS and SP compensations are more advantageous for a high-power transmission [7], [55].

Therefore SS and SP compensations are suitable for high power from an economic point of view. The PS or

PP compensations are typically used for a high power current source driven cables that run over a long distance [7].

But it is not a rule to use this topology only at a high power. The SS compensation is used and intensively investigated at different resonance frequencies from kilohertz [49], [58]–[69] to megahertz [70]–[72], and power from several watts [62], [72], [73] to tens of kilowatts [21], [55], [74].

However, with a power of several kilowatts and tens of kilowatts, the size of the coils must necessarily be increased with all compensation topologies, in order to have sufficient cooling area. For some WPT applications (for example in biomedicine), the temperature of the device should not exceed certain safe ranges.

The SP topology requires less secondary inductance than the SS one, it is an important advantage (Fig.8) [40]. Respectively, at the same time, a larger primary capacity needed [50], [75], [76].
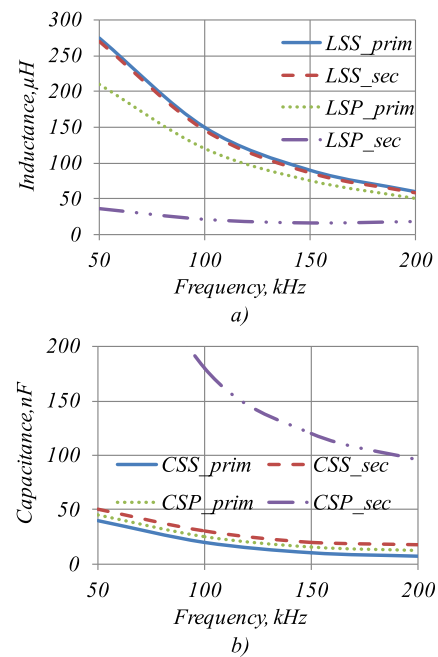

FIGURE 8. Comparison values for SS and SP topologies: a) required inductance; b) required capacitance [40].

From Fig.8, the smaller resonance frequency is, the greater the advantage of SP topology in the size of the secondary coil will be. The primary inductances in two topologies are almost identical.

This feature of SP topology is advisable to use in biomedical and other compact devices, such as wireless charging for a low-power transport [77]. The SP topology is recommended to be used in biomedical applications, or any application where a constant voltage transfer ratio without the necessity for feedback control is desired [78], [79].

The smaller size of the secondary inductance will be better in the planar approach for combining all the magnetic components, when all the inductances are mutually solved and the compact size is very important [80].

The major drawback of the SS topology occurs at the light load condition, and when the receiver is not present and the equivalent impedance seen is zero at the primary resonance frequency with only the parasitic impedance of the capacitor and inductor limiting the current [7]. Also the disadvantage of the SS compensation method is the load dependency of the voltage transfer ratio, which could complicate the control and reduce the partial-load efficiency of the system [40].

An important criterion is the compensation behavior when changing the position of the coils. The misalignment behavior of basic topologies are considered in [56].

The basic compensation topologies are shown in Fig.6, and their misalignment behavior has been studied for the 2 kW IPT systems [55], [56]–Fig.9.
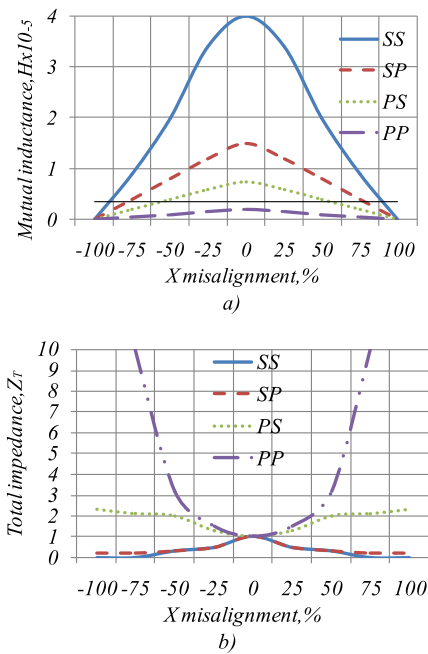

FIGURE 9. Variation with misalignment for the basic compensation topologies: a) of mutual inductance; b) of total impedance [56].

If the coils are not properly aligned, the mutual inductance coefficient decreases (Fig. 9a), modifying the total impedance (Table 3) of the system seen by the source (Fig. 9b). In the SS (5) and SP topologies (6), the total impedance decreases, causing an increase in both the current supplied to the load and the one supplied by the source. In the PS (7) and PP (8) topologies, the total impedance increases with the misalignment, causing a quick fall of both supplied and absorbed currents.

As it has been noted, the SS compensation is independent of the coupling coefficient, and the output current does not depend on the load on the resonance frequency [40].

Consequently the system exhibits a low sensitivity to the coil misalignment, and the resonant frequency of the resonant circuit is constant if there is no component tolerances.

The secondary side using the series compensation, namely the SS or PS, achieves a much smaller average absolute value

of the phase of the primary input impedance than that of using the parallel compensation, SP or PP [52].

In the SS topology, zero-voltage switching is ensured in the primary side switches by keeping the input impedance of the converter inductive while the output diodes are turned on at zero current and turned off at zero current. Because if there is soft-switching in all switches, very high frequency operation is possible [42].

For a constant magnetic coupling system, the magnitude of the output voltage of the SP topology IPT depends on the magnitude of the primary current which can be controlled by the primary input voltage [82]. In the SP topology with an increase of mutual inductance the efficiency of the system increases [7], [81].

The conducted analysis [83] determined that the performance of parallel topology on the secondary side with a significant load is better than in a series topology.

When the separating value of the load resistance R'_L is lower than the impedance of the resonant capacitor on the secondary side Z_{Cs}, the SS topology is much better, although in a rather narrow range of loads. The characteristics in Fig. 10 are dramatically reduced. On the contrary, at a high load resistance, the SP topology is preferable because of the fact that the impedance of the secondary resonant capacitor Z_{Cs} prevails over the parallel impedances R'_L and Z_{Cs}. The impedance of this capacitor is approximately equal to the load impedance R'_L (9).
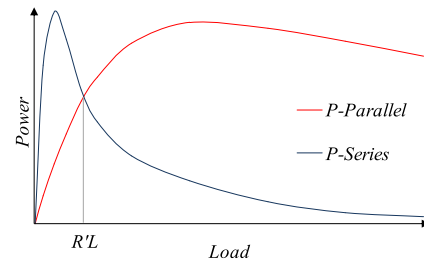

FIGURE 10. Waveform of output power dependence on load for SS and SP topologies [83].

From [83], the separating value of the load resistance R'_L can be expressed:

$$R'_L \approx Z_{Cs} = R_C + X_C = R_C + \frac{1}{2\pi F_r C_s}, \qquad (9)$$

where Z_{Cs} – impedance of a secondary capacitor consisting of the active R_c and reactive X_c resistances.

The active resistance of the capacitor can be neglected, since its magnitude almost does not affect the result.

Consequently, in the SS topology, the advantage is a remarkable loading characteristic; the SP-topology also has a good transmission efficiency with a significant change in the load range [83]. Mathematically proved that for the above-mentioned analysis it does not matter which topology (serial or parallel) will be on the side of the transmitter.

As for the requirement for the modes of a constant output current or voltage, in the simplest case they can be achieved

TABLE 3. Total impedance for the four basic topologies [56] and load independent output condition [10].

Topo-logy	Equation	№ of for mula	Topo-logy	Equation	№ of for mula
SS	$Z_T = \left(R_1 + j(L_1\omega - \dfrac{1}{C_1\omega}) \right) + \dfrac{\omega^2 M^2}{\left(R_2 + R_L + j(L_2\omega - \dfrac{1}{C_2\omega}) \right)}$	5	Current LIO current for SS	$\omega = \omega_r = \dfrac{1}{\sqrt{L_p \cdot C_p}}$	10
SP	$Z_T = \left(R_1 + j(L_1\omega - \dfrac{1}{C_1\omega}) \right) + \dfrac{\omega^2 M^2}{\left(R_2 + jL_2\omega + \dfrac{R_L}{1 + jR_L C_2\omega} \right)}$	6	Voltage LIO for SS; current LIO for SP	$\omega_L = \sqrt{\dfrac{\omega_p^2 + \omega_s^2 - \Delta}{2\cdot(1-k^2)}}; \ \omega_H = \sqrt{\dfrac{\omega_p^2 + \omega_s^2 + \Delta}{2\cdot(1-k^2)}}$	11
PS	$Z_T = \dfrac{1}{(R_1 + jL_1\omega) + \dfrac{\omega^2 M^2}{\left(R_2 + R_L + j(L_2\omega - \dfrac{1}{C_2\omega}) \right)} + jC_1\omega}$	7	Voltage LIO for SP	$\omega = \sqrt{\dfrac{1}{C_p \cdot \left(L_p + \dfrac{M\cdot L_s}{M + L_s} \right)}}$	12
PP	$Z_T = \dfrac{1}{\dfrac{1}{(R_1 + jL_1\omega) + \dfrac{\omega^2 M^2 (1 + jR_L C_2\omega)}{\left(R_L + (R_2 + jL_2\omega)(1 + jR_L C_2\omega) \right)}} + jC_1\omega}$	8	Voltage LIO for PS; current LIO for PP [41]	$\omega = \dfrac{1}{\sqrt{L_s \cdot C_s \cdot (1-k^2)}}$	13

by switching compensation topologies. This can be done both on the primary and on the secondary side.

At certain operating frequencies and compensation parameters, it is possible to work in the mode of a constant current output or constant voltage output, which does not depend on the load change (the load independence output conditions). In the work of researchers [10] noted that with the help of the SS and SP topologies in both cases, the compensation can be realized with the current or voltage Load Independence Output (LIO). At the two operating frequencies in the SP topology, can be implement a mode in which the output current will not depend on the load.

For the SS compensation, one frequency at which the current LIO mode works is detected and determined in [10], [41]. It is very convenient that it is equal to the resonant frequency and depends only on the parameters of the primary compensation (10). For operation in the voltage LIO mode, there are two frequencies (lower ω_L and upper ω_H) (11) in Table 3, where Δ is the correction factor, k is the coupling coefficient. For the SP compensation work in the voltage LIO will be (12), and work in the current LIO mode will be (11).

In [41], a simplified frequency value for the LIO was given. For the PS and PP topologies for the LIO conditions the expression (13) will be actual. At this frequency, the PS topology will work in the mode of the voltage LIO, and the PP in the current LIO mode. As a drawback, it can be noted that for the PS and PP topologies, there are no frequencies

for operating in the current LIO and voltage LIO modes, respectively [41].

The maximum efficiency condition for all basic compensation is achieved approximately at a secondary resonant frequency (14).

$$\omega_{\max} = \frac{1}{\sqrt{L_s \cdot C_s}}, \qquad (14)$$

For the parallel compensation the maximum efficiency depends on the coupling coefficient [41]. The maximum load power condition has different frequencies (Table 3). For the SS compensation it is (10) [6] and (14), for the SP it is (14), for PS is (13), for the PP approximately also is (13) [41].

Consequently, according to this analysis, the SS and SP compensations can provide a constant voltage and constant current output, but operate at different frequencies. For the wireless charging of electric vehicles for the operation in the current LIO mode, using the SS compensation, and for operation in the voltage LIO mode it is the SP [84], [85].

From the other article of these authors [84] as an extension to the experimental verification, it is determined that in the SS-topology for the implementation of voltage LIO, there will be two operating frequencies, as previously described (11) (at the resonance frequency 200 kHz). The maximum efficiency for the SS compensation can be achieved at a higher frequency (Fig.11). However, the performance and transfer coefficient will be slightly better with the SP topology. Important in this case is a soft switching
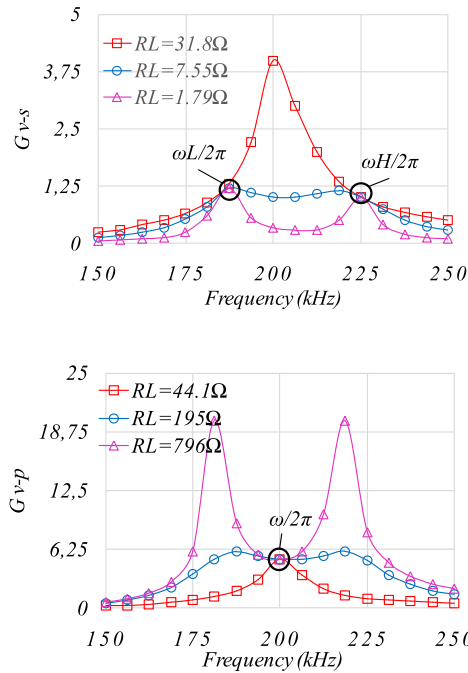
FIGURE 11. The transfer function for: a)SS topology; b)SP topology [84].

(a soft switching of the transistors in the inverter), which reduces the losses when also switching in the rectifier diodes. Although, when the compensation circuit works with a high efficiency and in the voltage LIO mode, a soft switching occurs automatically [84]. At the same time, it is possible to work efficiently at high frequencies up to a megahertz range [8].

Fig.11 shows the simulations results of a power transfer under different load conditions for the SS and SP compensations.

With a parallel compensating capacitor on the secondary side, there is one operating frequency for the implementation of the voltage LIO.

One of the main application of the LIO is to provide the CC and CV modes. In [50] it is shown that when a primary-side resonant current is maintained constant, the secondary-side series compensation performs as a voltage source, while the parallel compensation acts as a current source. Hence, the SS and SP compensations provide a possibility to realize the CC and CV charging for the variable load through adjusting the primary-side resonant current. In [10], [68], and [86]–[88] it is pointed that both the SS and SP compensations achieve CC/CV charging by choosing a suitable system operating frequency.

Another advantage of the series secondary compensation is that on the resonant frequency a series compensated secondary has a zero reflected reactance ImZrr (15), whereas a parallel-compensated system reflects a capacitive load (Table 4) [28].

In the case of parallel secondary compensation, the reflected reactance is present, but this can be adjusted as this value does not depend on the load (16). It can be shown (15) that both the reflected resistance ReZrr and the power transfer

capability assuming the constant primary current for the series compensation increase to infinity when the load is reduced to zero.

A similar result arises for parallel-compensated systems as the load increases to infinity [28]. This is one of the major differences between the series and parallel-compensated secondary systems.

For a series-compensated primary the load resistance is identical to the reflected resistance. The load reactance, however, depends on the primary capacitance and inductance, and also the reflected reactance. For a parallel-compensated primary the load conductance depends on the primary inductance, and also the reflected resistance and reactance, while the load susceptance depends on the primary capacitance and inductance as well as the reflected resistance and reactance [28]. Also secondary-side compensation topologies investigated in [89], where depicted main values dependencies that confirmed conclusions in this section.

Another criterion is an effect of zero or a weak coupling coefficient on the voltage and current stress [7]. The absence of the magnetic coupling happens when there is a misalignment or secondary coil. In this case, the compensation network should guarantee a safe operation of the WPT system. To allow zero or a weak coupling condition, the input impedance of the system should be infinite for the current source input and zero for the voltage source input [41]. Zero coupling is not allowed only for the SS compensation.

Table 4 also shows the bifurcation criteria for basic topologies (17-19). Typically, the primary Q_P and secondary Q_S quality factor is more than one. The most simple condition in the PS topology is (19). If the primary quality is greater than the secondary, then the bifurcation does not occur.

TABLE 4. Reflected resistance ReZr0 and reactance ImZr0 and bifurcation criteria [28].

Topology	Equation	№ of formula
Series secondary compensation	$\mathrm{Re}Z_{rr}=\dfrac{\omega_r^2 \cdot M^2}{R}$; $\mathrm{Im}Z_{rr}=0$	15
Parallel secondary compensation	$\mathrm{Re}\,Z_{rr}=\dfrac{M^2 \cdot R}{L_s^2}$; $\mathrm{Im}\,Z_{rr}=-\dfrac{\omega_r^2 \cdot M^2}{L_s}$	16
SS	$Q_p > \dfrac{4Q_S^3}{4Q_S^2-1}$	17
SP&PP	$Q_p > Q_s + \dfrac{1}{Q_s}$	18
PS	$Q_p > Q_s$	19

In order to visualize and improve the perception of information, based on the results of the comparison Table 5, a petal diagram comparing the basic features of the basic topologies is constructed (Fig.12).

The larger the number in the diagram (further from the center) and the larger the area of the figure is, the better will
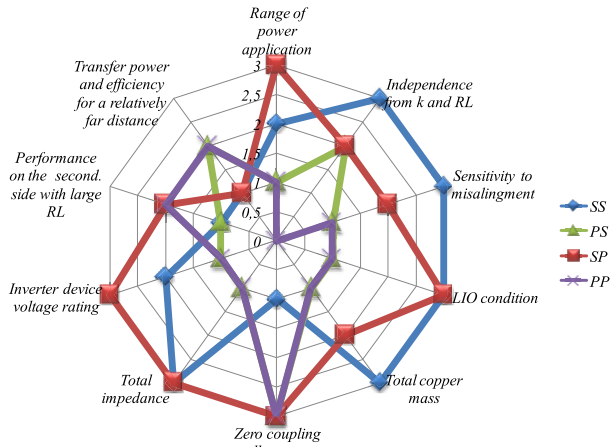
FIGURE 12. Petal diagram comparing basic topologies.

be the topology in comparison with others. The best are SS and SP topologies in the absolute majority of comparable parameters.

In conclusion, the work of the topologies at different frequencies is compared. The paper [90] compares 4 main topologies with 9 cases, also in the cases where there is only a primary or a secondary compensation.

The comparison among different topologies has been provided and it has been shown that the SS topology of the loosely coupled IPT system provides the best efficiency at 1 MHz frequency [52]. Also at 1 MHz the SS topology provides a higher power transfer than the SP [91], [92], but the SP has a slightly better efficiency. The effectiveness of the whole system increases with an increase in the coupling coefficient [91].

Table 5 presents a comparison of topologies based on the main parameters described in this section. For example, the table can be seen without an analysis of analytical expressions that if there is a parallel compensating capacitor on a certain side, then it depends on the change in the coupling coefficient and load. The benefits are marked with a green color, the drawbacks are red.

Also, the analysis of basic topologies and the calculation of main parameters was carried out in [93]–[95] and many others are not mentioned in this article.

Obviously, the knowledge about the features of the topologies and their work under different conditions and parameters is very important.

IV. MODIFICATION AND COMBINATION OF COMPENSATION TOPOLOGIES

Based on the classical basic compensation topologies (Fig.6), discussed in the previous section, other hybrid and more complex topologies are constructed.

A. MODIFICATION AND COMBINATION OF CLASSICS COMPENSATIONS TOPOLOGIES

They can be either combinations of two or more capacitors on one side (Fig.13f-h), or with the addition of series or parallel additional inductances (Fig.13a-e). Their features are

included in the Table 6. Other combinations with a parallel connection capacitance (C) and inductance (L) are possible.

The hybrid topologies (i.e. LCL-LCL, LCC-LCC) maintain high efficiency over their full range of coupling and loading [96]. However, the extra inductances and capacitances as well as their stray resistances in the hybrid topologies may cause much copper loss than the SS topology under the rated power, especially for the occasion of a high power transmission. The control complexity and the cost of the hybrid topologies are higher than those of the SS topology.

Despite this, the current source behaviors LCL-LCL and LCC-LCC topologies on the secondary side when operated with a voltage source inverter on the primary side make them be good candidates for the battery-charging applications [11], [97]. The equivalent impedance of capacitor and inductor has an opposite phase. The T circuit can be formed with either the LCL or CLC topology for the CC/CV mode in hybrid circuits for a massive electric bicycle charging [98], [99].

In [11] it is noted that the RMS output current of the double-sided LCC compensation topology is constant once the input voltage is fixed. By tuning the LCC compensation, Zero Current Switching (ZCS) can be achieved. Also, the LCC pickup can compensate the reactive power at the secondary side to form a unity power factor pickup. This compensation has the independence of the coupling coefficient and load conditions [100], [101]. The double-sided LCC compensation is the most popular as it can reduce the current stress in the inverter, has a high efficiency, high misalignment tolerance and load independence characteristics [11], [101]–[103].

The secondary side of the LCC compensation can be either a parallel compensation or series compensation. The parallel compensation is widely used due to its robustness to load variation [100]. The drawback of the parallel tuned system is in the transferred-impedance on the primary side which consists of both real and imaginary parts of the load. The series tuned pickup requires a large bridge rectifier capacitor to ensure a continuous conduction and the pickup voltage increases to a high value at large power levels [7], [101].

In [100] the LCC topology eliminates aforementioned problems and has the following advantages: lower losses in the rectifier, the pickup winding; the efficiency of the system is high as compared to the parallel pickup.

The advantages of the series primary resonant circuit are such as a supply stable voltage, and the blocking of dc component from the input voltage by a series capacitor. On the other hand, the large high-frequency current through a series capacitor will get the high capacitor voltage [104].

The parallel primary circuit offers a no–load regulation and a supply stable current but lacking of a dc component blocking. In the secondary side, the series secondary resonant circuit supplies the stable voltage and reflect only a real part of the impedance to the primary side.

The parallel secondary resonant circuit supplies the stable current which is suitable for battery charger. This circuit

TABLE 5. Comparison of four basic topologies and proposed application.

Parameter \ Topology		SS	SP	PS	PP
Independence on coupling coefficient and R_{Load}	Primary	Yes	Yes	No	No
	Secondary	Yes	No	Yes	No
Zero coupling allowance		Not allowed	Allowed	Allowed	Allowed
Total impedance		Decreases with misalignment	Decreases with misalignment	Increases with misalignment	Increases with misalignment
Sensitivity to coil misalignment		Low	Slightly larger than SS	High	High
Inverter device voltage rating		Lower dc link voltage (but higher than SP)	Lower dc link voltage	Higher voltage is needed as compared to SS and SP	Higher voltage is needed as compared to SS and SP
Total copper mass at 200kW [55]		Less copper mass than other	4.6% more than SS	30% more than SS	24% more than SS
Performance for low-power applications		Worse than parallel	Better than series	Worse than parallel	Better than series
Transfer power and efficiency for a relatively far distance between coils		Relatively low	Relatively low	Relatively high	Relatively high
Load independent output		Voltage and current	Voltage and current	Only voltage	Only current
Other advantages		1) The output current does not depend on the load on the resonance frequency. 2) Better efficiency and greater transmitted power at frequencies > 1MHz than in SP.	1) Requires a smaller receiver coil self-inductance than SS. 2) The parallel secondary resonant circuit supplies the stable current .	Not detected	Not detected
Other drawbacks		1) Load dependency of the voltage transfer ratio at partial-load condition. 2) Requires a lager receiver coil self-inductance than SP. 3) High-frequency current through series capacitor will get the high capacitor voltage.	Lacking of dc component blocking	1) Requires a current source input to avoid any instantaneous change in voltage 2) Large input resistance requires a high driving voltage to transfer sufficient amount of power.	1) A low power factor 2) A high load voltage of the parallel secondary . 3) Large current source requirements of the parallel primary. 4) Large input resistance requires a high driving voltage to transfer a sufficient amount of power.
Proposed application		1) Segmented dynamic WPT EV applications. 2) Static and dynamic WPT charger for EVs.	1)In biomedical applications. 2) For low-power transport or any application where a constant voltage transfer ratio without the necessity for feedback control is desired.	High-power application,EVs,buses	High-power application,EVs,buses
Proposed Power level usage		Preferable for a high-power IPT system	1) Low and middle power level. 2) For a high power from an economic point of view (less copper mass compared with PS and PP).	High power	High power

allows the reflection of both real and imaginary parts of the impedance to the primary side [104].

The resonant frequency would be changed when the load is varied. In practice, the load on the secondary side cannot model as a pure resistance and the non–linear load, increasing the system order. To combine the advantages of both simple resonant circuits, the LCL - LCCL resonant circuit is presented in [104].

However, the disadvantage of a dual side LCC compensation is a large volume [11]. A hybrid compensation topology by combining the series compensation and the LCC compensation with two additional switches is adopted in the receiver side [103] and in the transmitter [105] for the LCC-S topology.

Such a decision is a compromise with regard to the size and mass, with a preservation of almost these characteristics.

To compare a better classical compensation topology with a complex, the reference [106] is used, where comparisons of double-sided SS and LCC compensation are made. From Fig. 14 double-sided LCC compensation topology is

TABLE 6. Comparison of complex hybrid topologies and proposed application.

| Topology Parameter	LCL and its modifications	SP/S	S/SP	LCC and its modifications
Additional element on the side	2 inductances	1 capacitor	1 capacitor	1 inductance, 1 capacitor
Cost and size	High	Not high	Not high	Less size and cost than LCL system
Advantages	1) Maintaining a high efficiency over their full range of coupling and loading. 2) Remain high efficiency at low-quality factor Q 3) The VA rating is reduced 4)Lower losses in the rectifier, pickup winding	1) Output power can be maintained constant for a high misalignment. 2)Allows significantly higher positioning tolerance than a standard SS topology	1) Gain value is independent of the load change and the coupling coefficient. 2) Less circulating losses than SP under the condition of wide parameters variations.	1) Can achieve ZCS and ZPA operation at the same time 2) Independence of the coupling coefficient and load conditions 3) Can reduce the current stress in the inverter and compensate a reactive power on the secondary side. 4) High misalignment tolerance
Drawbacks	Transferred-impedance on the primary side consists of both real and imaginary parts of the load if the secondary side is parallel compensation	Combines disadvantages as in the secondary series compensation	No data	More complex tuning (control complexity)
Proposed application	WPT charger for EVs.	Mobile system battery charge	For a wide range of parameters as well as for high-power applications.	1)WPT charger for EVs; 2)a high-frequency application; 3) LCC SP compensation topology typically for multi-load WPT
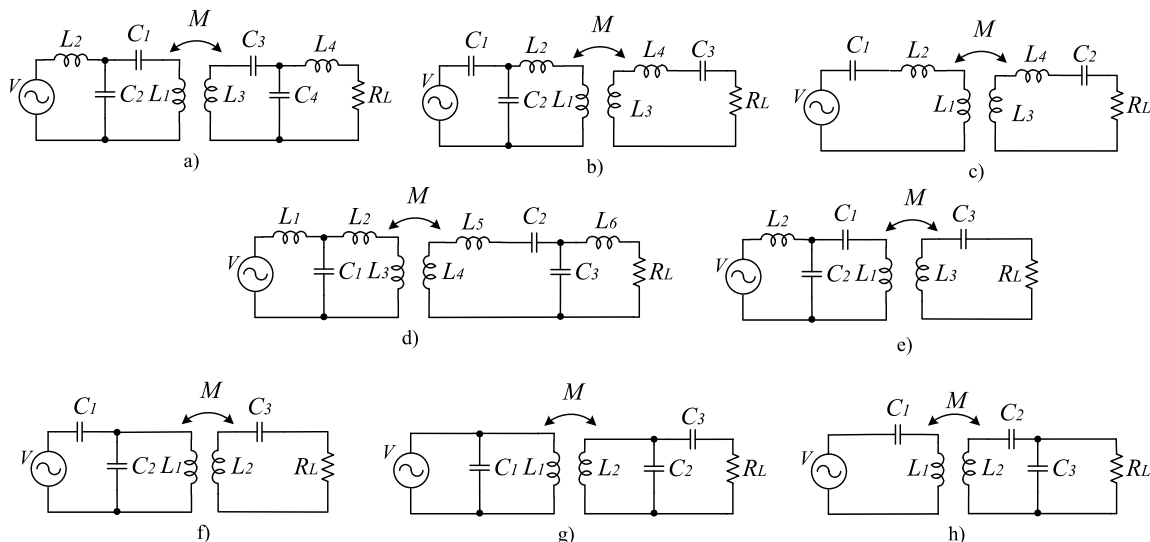
FIGURE 13. Some modified compensation topologies for IPT: a)LCC-LCC; b)CCL-LC; c)LC-LC; d)LCL-LCCL; e)LCC-S; f)SP-S; g)P-PS; h)S-SP.

less sensitive to the variation of coupling coefficient under ideal conditions. The voltage and current stresses on the series capacitors and main coils of the double-sided LCC compensation topology are smaller than SS compensation topology [106].

The efficiency of the double-sided LCC compensation topology is more stable at the more wide range distances than SS and it is keeping high on misalignment variable (Fig.15).

The secondary LCC and series compensation topologies are load independence and equal to one in ideal case and have a similar efficiency [89].

Certain topologies are positioned by the authors to ensure a high efficiency of the energy transfer and the VA rating can be

reduced. For example, at high frequencies greater than 1 MHz [107], for this purpose the LLC compensation is used on the primary side.

The high-order compensation topologies such as the LCC and LCL have become more and more popular due to the better comprehensive performance [100], [102], [108]–[110]. A fixed frequency control is usually adopted for the inverter with a double-sided LCC resonant topology. Consequently, an auxiliary switching power converter is required to control the output power.

Sometimes the WPT system or control method may depend on the topology of compensation. The paper [111] presents a novel control method that minimizes the need or use for a
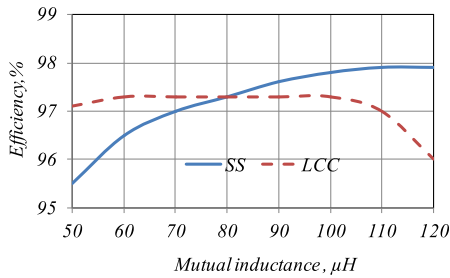
FIGURE 14. Comparison of the simulated efficiency between the double-sided SS and LCC compensation topologies at power 2.6 kW [106].
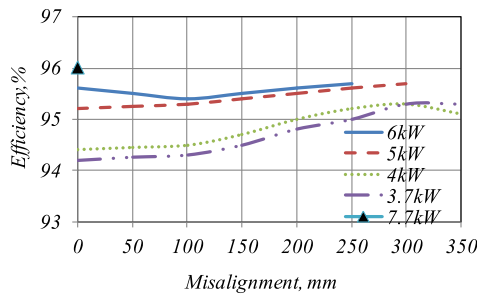

FIGURE 15. The experimental efficiency of LCC topology for different power levels with different misalignment [106].

number of components in a dual active bridge series LC-LC resonant converter topology. Efficiency of LC-LC topology may reach 92% [112].

In [113] the proposed LC-LC2 network (or S-CCL compensation) with efficiency 93% is reported. The LC-LC2 topology provides the input impedance with ZPA and voltage gain having load independent characteristics. Compared with S-SP topology, in this compensation the efficiency variation is less affected by the mutual inductance changing and higher-order harmonics not injected to the rectifier side [113].

It is well known that in the inductance-capacitance (LC) series resonance circuit, the voltage values on L and C are identical, while the phases are opposite [114]. The LC-S topology loss is approximately the same as in the LCL, but in this case there will be fewer elements. [115]. Thus the sum of the two voltage vectors is zero, and the withstand voltage of the input power source can be reduced. In the meantime, much of the reactive current is delivered between the inductance L and the capacitance C in the LC parallel resonance circuit. Hence, the load can receive more active power with the LC-P compensation.

In [116] the CCL transmitter and LC receiver (CCL/LC) are employed for the compensation. A parallel resonance is employed for a transmitter with the advantage of a lower circulating current from the power electronics circuit, as parallel capacitor forms a low impedance path for the circulating current.

To avoid compensating inductances, an additional capacitor should be used.

As noted in the previous section, the series compensation requires a higher voltage and current than the parallel compensation. Therefore, the SP combination is required to obtain the required capacitance in order to achieve the desired voltage and current ratings. The IPT system requires a perfect alignment of the coils to transfer the power with a high efficiency. The benefit of the SP/S compensation scheme is that the output power can be maintained constant for a high misalignment [56].

The SP/S compensation topology is presented in [56], which allows a significantly higher positioning tolerance than the standard SS topology. The SP/S topology combines the characteristics of the SS and PS configurations and is suitable for a mobile system battery charge, where a high misalignment may occur.

A novel S/SP type compensation contactless resonant converter is proposed in [86], which can realize the constant gain intersection point with a zero phase angle of the input impedance. Meanwhile, the constant gain value is independent of both the load change and the k. Another merit here is that the output voltage gain is not sensitive to the parameter change around the gain intersection point.

The S/SP type compensation can realize a good output stability and low circulating losses under the condition of wide parameters variations [117].

The output voltage gain of the S/S compensated converter at the full resonant frequency is proportional to the load, resulting in a wide output voltage variation. Thus, the S/S compensation cannot achieve a constant voltage gain at the zero input phase angle point.

The output voltage gain of the S/SP compensated converter is less sensitive to the variation of transformer's parameters than that of the SP compensated converter. Thus, the SP and the S/SP compensated converters can achieve both a constant gain and high efficiency at the full resonant frequency. Therefore, the S/SP compensation is suitable for a wide range of parameters as well as for high-power applications [117].

To improve the misalignment performance in PS, in [7] it is shown a compensation circuit that adds a series capacitor to the parallel resonant circuit (P/PS compensation). The PS-P compensation has efficiency 90% [118].

In addition to adding components to the classical topologies, a single sided compensation is also used: a primary S-compensation [34], secondary P-compensation [35], secondary S-compensation [37]. On the opposite side there will be no element responsible for the resonance.

A one-side primary capacitor compensation is proposed in [119]. In a resonant system with a high quality factor, this system could be regarded as a narrow band system. Therefore, the voltage on the primary inverter output is assumed a sinuous voltage and high order harmonics are neglected. The input current is also assumed a sinuous current without high order harmonics under a steady-state.

With the removal of the capacitor on the secondary coil, the effect of the reflected reactance is cancelled through a proper selection of the primary compensated

capacitor. This means that the problem of frequency deviation due to the reflected impedance from the secondary circuit is minimized [120]. The important advantages of the S-compensation include less component count and the complexity of the WPT system with an increased power transfer capability and less distortion on the primary current compared with the SS topology.

But a single sided compensation also has less regulated resonance parameters that can not provide a sufficient freedom to meet all the criteria for designing a WPT system [10], so it is rarely used in practical applications.

Taking into account many considered articles, the LCC and LCL compensations are better among complex compensation topologies and may reach efficiency more than 95% [19], [121], [122].

In the Table 6, a comparison of topologies based on the basic parameters described in this subsection is given. The benefits are marked with green color, the drawbacks are red.

B. COMPENSATION IN MULTIPLY INPUT AND OUTPUT SYSTEMS, MULTICOILS SYSTEMS

Most often in the works of researchers and in practical implementation there are circuits with two coils, the transmitting and receiving. They are called in some sources Single-Input-Single-Output (SISO)-Fig.16a. But classical and modified compensation topologies are also used in the cases where there are several coils on the primary or on the secondary side. It is logical to assume that the more coils will be, the more complex the system will be, because the number of mutual inductances and the influence will be proportional to each [123].

FIGURE 16. Magnetic induction model for IPT: a)SISO; b)MISO; c)SIMO; d)MIMO [4].

At the same time, the parallel inclusion of several coils allows to reduce the overvoltage on semiconductor elements,

improve the shape of the sinusoidal voltage, and increase the maximum efficiency at a constant frequency. The key advantages of the three-coil system are the maximum energy efficiency, the energy efficiency stiffness against load variations and the reduced EMF emission induced by the coil misalignments [124], [125].

In [4] analytically described that the SISO model may be extended to Multiple-Input-Single-Output (MISO) – Fig.16b, Single-Input-Multiple-Output (SIMO) - Fig.16c and Multi-Input Multi-Output (MIMO) - Fig.16d configurations. In the examples below, the SS compensation is used as an illustration of the use of the compensation topology.

The S-S-S compensated three-coil (MISO) WPT system can achieve the CV characteristic [97], and the S-S-LCC compensated three-coil WPT system can achieve the CC characteristic. In addition, both of the two cases can realize Zero Phase Angle (ZPA).

Three-coil MISO system with the SSS compensation is used for a Z-source network [126]. Such Z-source system can operate in a wide range of voltage and depending on the topology it can work in two modes: buck and boost. It can work without a dead time for the switches as it is tolerant to the shoot-through states. This increases the overall reliability of a converter. Also, the same compensation topology is used in three-phase inverters, by a capacitor for each phase [127].

Such systems are used to transmit not only the energy but also information [128]. Wireless information and power transfer in a MISO downlink system consists of one multi-antenna transmitter, one single-antenna information receiver, multiple multi-antenna Eavesdroppers (EVES), and a multiple single-antenna Energy-harvesting Receivers (ERs).

Another example is the use of MISO systems with the basic compensation topologies for the dynamical charging EVs. In this case, the road surface is fitted with transmission coils, and in the vehicle floor is embedded a receiving coil [21], [57].

Three-coil MISO system is designed in [18]. On the primary side there are two series compensations. In the secondary side, the parallel LC connection is adopted to tune the resonant frequency. Since the parallel-connected LC circuit acts as a current source at a resonant frequency, a high voltage can be obtained, making it suitable for the voltage boosting.

Free-positioning SIMO systems with a coil array and a compensation allow multiple devices to be charged simultaneously irrespective of their positions (utilizes the whole charger surface for a power transfer without any restriction on the orientation of the secondary coil). Free-positioning approach can be applied based on the three-layer coil array structure [129]. This approach offers more user-friendliness, may also charge 1 to 3 smartphones [4]. The SIMO is also used for Maglev train with the series compensation on the primary side [130]; for the bidirectional Vehicle-To-Grid (V2G) systems multilevel IPT converters with 3 coils LCL compensation [131] and the load-isolation WPT with the 3-coil SSS compensation [132].
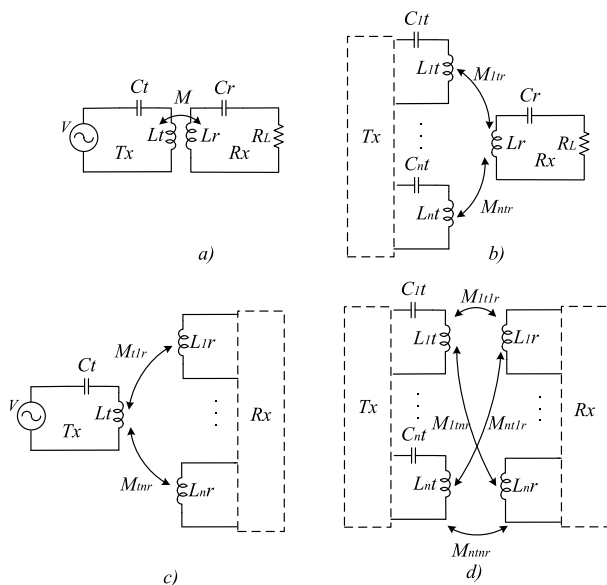
Three system models including the MISO, SIMO and MIMO are proposed in [133] to characterize the number of transmitters and receivers to the link. The MIMO is used for increasing the magnetic communication range [134]. The crosstalk between the transmit coils and the receive coils is small. The LCL-T compensation in [135] is used for a parallel inverter with the IPT to achieve a maximum efficiency at a high power (MIMO system).

The MISO, SIMO topologies with a compensation network are commonly used for improved shape of signals, bidirectional converters, a high voltage and power level, they help to unleash the power topology potential and provide highly efficient work, despite the size and cost.

V. APPLICATION OF COMPENSATION TOPOLOGIES IN IPT SCHEMES AND FUTURE DIRECTIONS FOR INVESTIGATIONS

In this section the important issues about the modern sphere of compensation topologies use for different applications in WPT schemes as well as possible future research directions in this area are considered.

A. APPLICATION OF COMPENSATION TOPOLOGIES

In some cases, researchers indicate for which applications the WPT system can be used (for example, the transmission of information [128], in some cases the systems are positioned as universal or simply this issue is not given attention to. The choice of the topology usually depends on the power, the size of the device, the gap between the coils and the variation of the load, etc. (Tables 4 and 6).

The general typical WPT scheme is shown in Figure 1b along with its brief review in the second section. The topologies of inverters and rectifiers may be different, that is out of scope in this article. A battery or resistive load often acts as a load.

As previously noted, SP topology is often used with high input and low output power. For all power levels, and especially for medium and high and with frequent variable load parameters and distance between coils, SS compensation is applied. For power of tens and hundreds of kilowatts with large input current, sometimes PS and PP compensations are used. If the changes in the output parameters are insignificant, then the combined compensation topologies can be used for high efficiency. Details are given below.

The most massive used area of the WPT systems with compensation are chargers of a varying power, mainly with the SS compensation. Less used are the LCC and LCL compensations [11], [104]. Charging can be static or dynamic. With a static charge of the coil, the transmitter and the receiver are in a stationary state opposite each other (Fig.17a). In the case of dynamic charging, a large number of transmission coils are installed on the road surface, and one receiver coil (mostly) is located on the vehicle (Fig.17b). The double sided LCL-LCL compensated MIMO system is used in dynamic charging [121]. At any moment of movement, the power transmitted must be constant. According to this

principle can be implemented not only the charge, but also the electric motor supply.

Speaking about a high power, it can be EVs, buses, trains [136]. The supply system of Maglev train is developed in [130]. In [21], [57] a detailed review of the kilowatt systems of static and dynamic charging of EVs (even LC-LC2 compensation [137]), electric buses, with the description and analytical expressions, the compensation and geometry of coils, efficiency, and others is given [2], [50], [138]. The development of such systems with experimental designs is shown in the example of the 5 kW EV charging system [38], [39], [139]. Sometimes the CPT is used to transmit the energy in the EVs, but as experimental prototypes [140].

In public transport systems [141] the secondary systems are electrically isolated and move along a long track. The WPT system has to provide the intervention free battery charging to a specially designed low weight electric vehicle for use in a national park. High-speed railway power system is shown in [142].

The SS topology is used in the high-power (more 1 kW) low voltage (less 100 V) chargers [60], [143]. Also designed 3.7 kW systems for Light-Duty Vehicles are described in [144]. The SS topology is most suitable for EV charging [145] in view of the benefits described in Section IV.

The same principles are used for charging scooters [47], electric bikes (Fig.17c) [11], [81], [105], [77], [98], [99], [147] and other low-power transport devices. There may be charging stations for charging multiple bicycles at different power levels with the LCL and CLC compensation [98], [99].

In industry there are SP-compensated material handling systems [53], [148]. The WPT system is used for a robot manipulation application [36]. In such cases, rotary coils are often used to have more degrees of freedom in the mechanism [42], [149].

It is also possible to use for the WPT by the resonance and inductive methods from renewable energy sources [48] – used the PS topology, [150], [151] - a contactless underwater power delivery.

Researchers developed an 8-resonator system, in which the series resonant topology was used in both the transmitter and receiver. The Domino resonator systems are a reproduction of Nikola Tesla's experiments [152].

For portable or implantable and biomedical applications in most cases, the SP or SS topology is used commonly [153], [154]. Preferably these are medical implants [29], [155].

For example, a leadless pacemaker charged by wireless electricity is depicted in Fig.17g [24]. Even before the era of smartphones, prototypes of universal-input battery chargers for mobile phones were developed [156]. The most modern option is a mobile phone charger [157] with the SS compensation. Fig.17e shows one of the many existing devices for simultaneous charging of several smartphones [4], [158], [160].

A large group consists of consumer electronics of a different designation and power, a car seat power [158], the LED lighting [159], household devices (TV, monitors,
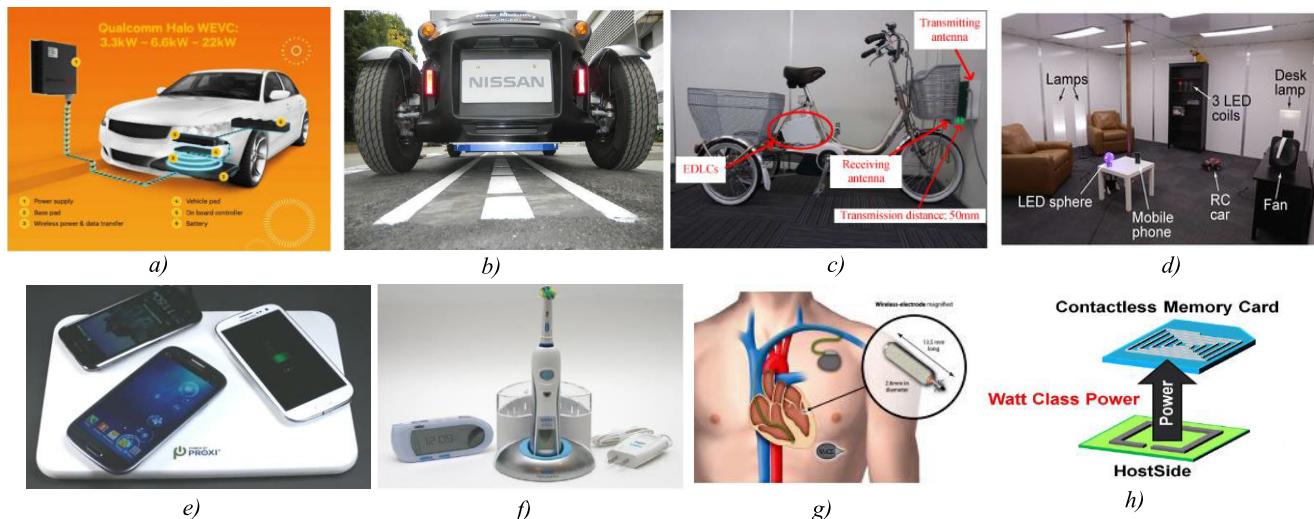
FIGURE 17. Some examples of using IPT with a resonant coupling: a) stationary charging for EV [21]; b) wireless dynamic charging of EV (roadway powered) [161]; c) bicycle charger [147]; d) powering multiple wireless devices revealing a practical living room environment [24]; e)mobile charger [158]; f) electric toothbrush charger [24]; g) leadless pacemaker charged by wireless electricity [24]; h) contactless memory card (RFID) [18].

toothbrushes (Fig.17f), and portable devices [35], [111] with LC-LC compensation). The power supply can be as for a certain device and as for all household devices in the room (Fig.17d) [24].

The proposed SP-compensation topology in the WPT scheme for contactless memory cards at a frequency of 6.78 MHz is in Fig.17h [18].

For distances of several meters and kilometers are used far-field charging systems, which can be realized through either a non-directive Radio Frequency (RF) radiation or a directive RF beamforming. This is Radio Frequency IDentification (RFID), Wireless Body Area Networks (WBANs), Global System for Mobile Communications (GSM) bands, and many others. A very detailed study of this issue and the above-mentioned applications has been conducted [4]. The scope of using the WPT systems with different topologies of compensation is extensive, constantly increasing and affecting most areas of human life and work. The progress of the global economy promotes the implementation of researchers' laboratory developments in industrial and commercial devices.

B. FUTURE DIRECTIONS AND FURTHER INVESTIGATIONS OF COMPENSATION TOPOLOGIES

The main direction of the use and development of the compensation topologies is to increase the efficiency, reduce overall cost and size. It can be achieved by several ways, in particular:

1) Using of high-frequency multilevel/multi-pulse converters with multicoils structure (MISO, SIMO, MIMO) and combined compensation topologies;

2) Reduce parasitic capacities in coils, which will lead to the possibility of work at high resonance frequency and increase the effective distance of the wireless transmission of the energy [122];

Despite the above-mentioned directions of development and improvement of compensation topologies, the analysis of recent publications also revealed a certain developmental crisis and almost complete study of various topologies of compensation.

At the same time, for a significant cost and size reduction, along with improving overall efficiency of the WPT systems, the following directions can be emphasized:

1) Research of new high-frequency magnetic and shielding materials, printed planar coils and design of coil shapes for a precise direction of magnetic flux;

2) Research of existing prospective and new high-frequency semiconductor materials with the improved dynamic properties;

3) Develop and implement the new standards for work frequencies.

VI. CONCLUSION

The IPT systems are becoming increasingly popular in the research area, in particular in the wireless battery charging applications. This paper has presented the comprehensive analytical review of compensation topologies in the IPT.

This study is focused on the main types of compensation circuits and their derivations. The topologies with the series placement of the primary compensating capacitor are the most effective in the IPT for charging devices among the four classical schemes and may reach up to 97% of the efficiency. It has been established that the SS and SP topologies will be the most optimal for most of the parameters from all topologies for most applications and for different power levels. The SS topology is recommended for the unit turns ration between the primary and secondary coils. It does not depend neither on the magnetic coupling coefficient or the load on the resonance frequency. At the same time, the SP

solution is recommended in case of the low output voltage. The minimum size of a secondary side coil is achievable, but the primary side requires the additional tuning in case of distance changing.

The compensation topologies with a parallel primary connection are recommended only for a high power application.

Among the modified topologies, the combination of the LCC and LCL in WPT systems is better than others and reached efficiency more 95% in a certain operation point.

The main direction of the development of compensation topologies is to increase the frequency of the resonant link. Considerable attention will be paid to the research of new high-frequency magnetics and semiconductor materials with improved characteristics. A promising direction is also the use of combined and classical compensation topologies in multilevel/multi-pulse converters with multicoils structure.

REFERENCES

[1] C. Xia, Y. Zhou, J. Zhang, and C. Li, "Comparison of power transfer characteristics between CPT and IPT system and mutual inductance optimization for IPT system," *J. Comput.*, vol. 7, no. 11, pp. 2734–2741, 2012.

[2] F. Musavi and W. Eberle, "Overview of wireless power transfer technologies for electric vehicle battery charging," *IET Power Electron.*, vol. 7, no. 1, pp. 60–66, Jan. 2014.

[3] I. Korotyeyev, I. V. Pentegov, R. Strzelecki, and I. V. Volkov, "Badanie procesów tesli w wybranych układach prostownikowych," in *Proc. Podstawowe Problemy Energoelektroniki Elektromechaniki (PPEE), Materiały Sympozjum*, Wisła, Polska, 2000, pp. 375–378.

[4] X. Lu, P. Wang, D. Niyato, D. I. Kim, and Z. Han, "Wireless charging technologies: Fundamentals, standards, and network applications," *IEEE Commun. Surveys Tuts.*, vol. 18, no. 2, pp. 1413–1452, 2nd Quart., 2016.

[5] J. D. Jackson, *Classical Electrodynamics*, 3rd ed. New York, NY, USA: Wiley, 1999.

[6] M. H. Ameri, A. Y. Varjani, and M. Mohamadian, "A new maximum inductive power transmission capacity tracking method," *J. Power Electron.*, vol. 16, no. 6, pp. 2202–2211, Nov. 2016.

[7] D. Patil, M. K. McDonough, J. M. Miller, B. Fahimi, and P. T. Balsara, "Wireless power transfer for vehicular applications: Overview and challenges," *IEEE Trans. Transport. Electrific.*, vol. 4, no. 1, pp. 3–37, Mar. 2018.

[8] Z. U. Zahid, C. Zheng, R. Chen, W. E. Faraci, J.-S. J. Lai, M. Senesky, and D. Anderson, "Design and control of a single-stage large air-gapped transformer isolated battery charger for wide-range output voltage for EV applications," in *Proc. IEEE Energy Convers. Congr. Expo.*, Denver, CO, USA, Sep. 2013, pp. 5481–5487.

[9] B. L. Cannon, J. F. Hoburg, D. D. Stancil, and S. C. Goldstein, "Magnetic resonant coupling as a potential means for wireless power transfer to multiple small receivers," *IEEE Trans. Power Electron.*, vol. 24, no. 7, pp. 1819–1825, Jul. 2009.

[10] W. Zhang and C. C. Mi, "Compensation topologies of high-power wireless power transfer systems," *IEEE Trans. Veh. Technol.*, vol. 65, no. 6, pp. 4768–4778, Jun. 2015.

[11] T. Kan, T.-D. Nguyen, J. C. White, R. K. Malhan, and C. C. Mi, "A new integration method for an electric vehicle wireless charging system using LCC compensation topology: Analysis and design," *IEEE Trans. Power Electron.*, vol. 32, no. 2, pp. 1638–1650, Feb. 2017.

[12] *Wireless Power Transfer for Light-Duty Plug-in/Electric Vehicles and Alignment Methodology*, Standard J2954_201904, SAE, 2016. [Online]. Available: http://standards.sae.org/wip/j2954/

[13] D. Kettles, *Electric Vehicle Charging Technology Analysis And Standards*, Standard FSEC-CR-1996-15, 2015. [Online]. Available: http://www.fsec.ucf.edu/en /publications/pdf/FSEC-CR-1996-15.pdf

[14] *On-Line Electric Vehicle (OLEV) Project and Vehicular Wireless Power Transfer Technology*. [Online]. Available: http://greentechlatvia.eu/wp-content/uploads/bsk-pdf-manager/2-5a_OLEV_Project_and_Technology_(Ahn)_rev_a_15.pdf

[15] X. Lu, D. Niyato, P. Wang, D. I. Kim, and Z. Han, "Wireless charger networking for mobile devices: Fundamentals, standards, and applications," *IEEE Wireless Commun.*, vol. 22, no. 2, pp. 126–135, Apr. 2015.

[16] Qi [Electronic Resource]. *Wireless Power Consortium*. [Online]. Available: https://www.wirelesspowerconsortium.com

[17] K. Finkenzeller, *RFID Handbook*, 2nd ed. New York, NY, USA: Wiley, 2003, pp. 161–181.

[18] K. Tomita, R. Shinoda, T. Kuroda, and H. Ishikuro, "1-W 3.3–16.3-V boosting wireless power transfer circuits with vector summing power controller," *IEEE J. Solid-State Circuits*, vol. 47, no. 11, pp. 2576–2585, Nov. 2012.

[19] M. A. Houran, X. Yang, and W. Chen, "Magnetically coupled resonance WPT: Review of compensation topologies, resonator structures with misalignment, and EMI diagnostics," *Electronics*, vol. 7, no. 11, p. 296, 2018.

[20] R. Tseng, B. von Novak, S. Shevde, and K. A. Grajski, "Introduction to the alliance for wireless power loosely-coupled wireless power transfer system specification version 1.0," in *Proc. IEEE Wireless Power Transf. (WPT)*, Perugia, Italy, May 2013, pp. 79–83.

[21] C. T. Rim, *Practical Design of Wireless Electric Vehicles: Dynamic & Stationary Charging Technologies*. 2017.

[22] *Review and Evaluation of Wireless Power Transfer (WPT) for Electric Transit Applications*. [Online]. Available: https://www.transit.dot.gov/sites/fta.dot.gov/files/FTA_Report_No._0060.pdf

[23] International Commission on Non-Ionizing Radiation Protection, "Guidelines for limiting exposure to time-varying electric and magnetic fields (1 Hz to 100 kHz)," *Health Phys.*, vol. 99, no. 6, pp. 818–836, 2010.

[24] M. Song, P. Belov, and P. Kapitanova, "Wireless power transfer inspired by the modern trends in electromagnetics," *Appl. Phys. Rev.*, vol. 4, no. 2, 2017, Art. no. 021102.

[25] *IEEE Standard for Military Workplaces–Force Health Protection Regarding Personnel Exposure to Electric, Magnetic, and Electromagnetic Fields, 0 Hz to 300 GHz*, IEEE Standard C95.1-2345, May 2014.

[26] K. Aditya and S. S. Williamson, "Design considerations for loosely coupled inductive power transfer (IPT) system for electric vehicle battery charging—A comprehensive review," in *Proc. IEEE Transp. Electrific. Conf. Expo (ITEC)*, Dearborn, MI, USA, Jun. 2014, pp. 1–6.

[27] R. C. Fernandes and A. A. de Oliveira, "Theoretical bifurcation boundaries for Wireless Power Transfer converters," in *Proc. IEEE 13th Brazilian Power Electron. Conf. 1st Southern Power Electron. Conf. (COBEP/SPEC)*, Fortaleza, Brazil, Nov./Dec. 2015, pp. 1–4.

[28] C.-S. Wang, G. A. Covic, and O. H. Stielau, "Power transfer capability and bifurcation phenomena of loosely coupled inductive power transfer systems," *IEEE Trans. Ind. Electron.*, vol. 51, no. 1, pp. 148–157, Feb. 2004.

[29] G. B. Joun and B. H. Cho, "An energy transmission system for an artificial heart using leakage inductance compensation of transcutaneous transformer," *IEEE Trans. Power Electron.*, vol. 13, no. 6, pp. 1013–1022, Nov. 1998.

[30] T. Bieler, M. Perrottet, V. Nguyen, and Y. Perriard, "Contactless power and information transmission," in *Proc. IEEE-IAS Annu. Meeting Conf. Rec.*, vol. 1, Sep./Oct. 2001, pp. 83–88.

[31] H. Sakamoto, K. Harada, S. Washimiya, K. Takehara, Y. Matsuo, and F. Nakao, "Large air-gap coupler for inductive charger [for electric vehicles]," *IEEE Trans. Magn.*, vol. 35, no. 5, pp. 3526–3528, Sep. 1999.

[32] J. Lukacs, M. Kiss, I. Nagy, G. Gonter, R. Hadik, K. Kaszap, and A. Tarsoly, "Inductive energy collection for electric vehicles," in *Proc. 4th Power Electron. Conf.*, Budapest, Hungary, 1981, pp. 71–81.

[33] K. Lashkari, S. E. Schladover, and E. H. Lechner, "Inductive power transfer to an electric vehicle," in *Proc. 8th Int. Vehicle Symp.*, 1986, pp. 258–267.

[34] J. M. Barnard, J. A. Ferreira, and J. D. van Wyk, "Sliding transformers for linear contactless power delivery," *IEEE Trans. Ind. Electron.*, vol. 44, no. 6, pp. 774–779, Dec. 1997.

[35] H. Abe, H. Sakamoto, and K. Harada, "A noncontact charger using a resonant converter with parallel capacitor of the secondary coil," *IEEE Trans. Ind. Appl.*, vol. 36, no. 2, pp. 444–451, Mar. 2000.

[36] A. Kawamura, K. Ishioka, and J. Hirai, "Wireless transmission of power and information through one high frequency resonant AC link inverter for robot manipulator applications," in *Proc. 13th IEEE Ind. Appl. Conf. Meeting Conf. Rec. (IAS)*, vol. 3, Oct. 1995, pp. 2367–2372.

[37] A. Kurs, A. Karalis, R. Moffatt, J. D. Joannopoulos, P. Fisher, and M. Soljačić, "Wireless power transfer via strongly coupled magnetic resonances," *Science*, vol. 317, no. 5834, pp. 83–86, Jun. 2007.

[38] F. Liu, Z. Zhao, K. Chen, J. Nie, Y. Zhang, and L. Yuan, "Comparative study of current control methods for a 5 kW wireless EV charging system," in *Proc. IEEE 2nd Annu. Southern Power Electron. Conf. (SPEC)*, Auckland, New Zealand, Dec. 2016, pp. 1–5.

[39] R. Bosshard, J. W. Kolar, and B. Wunsch, "Accurate finite-element modeling and experimental verification of inductive power transfer coil design," in *Proc. IEEE Appl. Power Electron. Conf. Expo. (APEC)*, Fort Worth, TX, USA, Mar. 2014, pp. 1648–1653.

[40] R. Bosshard, J. W. Kolar, J. Mühlethaler, I. Stevanović, B. Wunsch, and F. Canales, "Modeling and η-α-Pareto optimization of inductive power transfer coils for electric vehicles," *IEEE J. Emerg. Sel. Topics Power Electron.*, vol. 3, no. 1, pp. 50–64, Mar. 2015.

[41] Y. H. Sohn, B. H. Choi, E. S. Lee, G. C. Lim, G. H. Cho, and C. T. Rim, "General unified analyses of two-capacitor inductive power transfer systems: Equivalence of current-source SS and SP compensations," *IEEE Trans. Power Electron.*, vol. 30, no. 11, pp. 6030–6045, Nov. 2015.

[42] A. J. Moradewicz and M. P. Kazmierkowski, "Contactless energy transfer system with FPGA-controlled resonant converter," *IEEE Trans. Ind. Electron.*, vol. 57, no. 9, pp. 3181–3190, Sep. 2010.

[43] O. H. Stielau and G. A. Covic, "Design of loosely coupled inductive power transfer systems," in *Proc. Int. Conf. Power Syst. Technol. (PowerCon)*, vol. 1. Dec. 2000, pp. 85–90.

[44] R. Ota, N. Hoshi, and J. Haruna, "Design of compensation capacitor in S/P topology of inductive power transfer system with buck or boost converter on secondary side," *IEEJ J. Ind. Appl.*, vol. 4, no. 4, pp. 476–485, 2015.

[45] H. Movagharnejad and A. Mertens, "Design metrics of compensation methods for contactless charging of electric vehicles," in *Proc. 19th Eur. Conf. Power Electron. Appl. (EPE ECCE Eur.)*, Warsaw, Poland, Sep. 2017, pp. P.1–P.10.

[46] S.-H. Lee and R. D. Lorenz, "Development and validation of model for 95%-efficiency 220-W wireless power transfer over a 30-cm air gap," *IEEE Trans. Ind. Appl.*, vol. 47, no. 6, pp. 2495–2504, Nov./Dec. 2011.

[47] J.-S. Tsai, J.-S. Hu, S.-L. Chen, and X. Huang, "Directional antenna design for wireless power transfer system in electric scooters," *Adv. Mech. Eng.*, vol. 8, no. 2, pp. 1–13, 2016.

[48] S. Samanta and A. K. Rathore, "Wireless power transfer technology using full-bridge current-fed topology for medium power applications," *IET Power Electron.*, vol. 9, no. 9, pp. 1903–1913, Jul. 2016.

[49] H. Li, J. Li, K. Wang, W. Chen, and X. Yang, "A maximum efficiency point tracking control scheme for wireless power transfer systems using magnetic resonant coupling," *IEEE Trans. Power Electron.*, vol. 30, no. 7, pp. 3998–4008, Jul. 2015.

[50] C.-S. Wang, O. H. Stielau, and G. A. Covic, "Design considerations for a contactless electric vehicle battery charger," *IEEE Trans. Ind. Electron.*, vol. 52, no. 5, pp. 1308–1314, Oct. 2005.

[51] W. Zhang, S.-C. Wong, C. K. Tse, and Q. Chen, "An optimized track length in roadway inductive power transfer systems," *IEEE J. Emerg. Sel. Topics Power Electron.*, vol. 2, no. 3, pp. 598–608, Sep. 2014.

[52] M. Fu, Z. Tang, and C. Ma, "Analysis and optimized design of compensation capacitors for a megahertz WPT system using full-bridge rectifier," *IEEE Trans. Ind. Informat.*, vol. 15, no. 1, pp. 95–104, Jan. 2019.

[53] J. T. Boys, G. A. Covic, and A. W. Green, "Stability and control of inductively coupled power transfer systems," *IEE Proc.-Electr. Power Appl.*, vol. 147, no. 1, pp. 37–43, Jan. 2000.

[54] H. Hong, D. Yang, and S. Won, "The analysis for selecting compensating capacitances of two-coil resonant wireless power transfer system," in *Proc. IEEE Int. Conf. Energy Internet (ICEI)*, Beijing, China, Apr. 2017, pp. 220–225.

[55] J. Sallan, J. L. Villa, A. Llombart, and J. F. Sanz, "Optimal design of ICPT systems applied to electric vehicle battery charge," *IEEE Trans. Ind. Electron.*, vol. 56, no. 6, pp. 2140–2149, Jun. 2009.

[56] J. L. Villa, J. Sallan, J. F. S. Osorio, and A. Llombart, "High-misalignment tolerant compensation topology for ICPT systems," *IEEE Trans. Ind. Electron.*, vol. 59, no. 2, pp. 945–951, Feb. 2012.

[57] R. Bosshard and J. W. Kolar, "Inductive power transfer for electric vehicle charging: Technical challenges and tradeoffs," *IEEE Power Electron. Mag.*, vol. 3, no. 3, pp. 22–30, Sep. 2016.

[58] N. Femia, G. Di Capua, and G. Lisi, "Power vs efficiency analysis in high-frequency wireless power transfer systems—Part I: Model," in *Proc. IEEE 2nd Int. Forum Res. Technol. Soc. Ind. Leveraging Better Tomorrow (RTSI)*, Bologna, Italy, Sep. 2016, pp. 1–5.

[59] C. Anyapo, N. Teerakawanich, and C. Mitsantisuk, "Phase-shift phase-lock loop (PLL) control for wireless power transmission system using primary-side information," in *Proc. Int. Electr. Eng. Congr. (iEECON)*, Pattaya, Thailand, Mar. 2017, pp. 1–4.

[60] M. Petersen and F. W. Fuchs, "Design of a highly efficient inductive power transfer (IPT) system for low voltage applications," in *Proc. PCIM Eur., Int. Exhib. Conf. Power Electron., Intell. Motion, Renew. Energy Energy Manage.*, Nuremberg, Germany, May 2015, pp. 1–8.

[61] X. Liu, J. Liu, J. Wang, C. Wang, and X. Yuan, "Design method for the coil-system and the soft switching technology for high-frequency and high-efficiency wireless power transfer systems," *Energies*, vol. 11, no. 1, p. 7, 2018.

[62] A. Berger, M. Agostinelli, S. Vesti, J. A. Oliver, J. A. Cobos, and M. Huemer, "A wireless charging system applying phase-shift and amplitude control to maximize efficiency and extractable power," *IEEE Trans. Power Electron.*, vol. 30, no. 11, pp. 6338–6348, Nov. 2015.

[63] Y. Jiang, J. Liu, X. Hu, L. Wang, Y. Wang, and G. Ning, "An optimized frequency and phase shift control strategy for constant current charging and zero voltage switching operation in series-series compensated wireless power transmission," in *Proc. IEEE Energy Convers. Congr. Expo. (ECCE)*, Cincinnati, OH, USA, Oct. 2017, pp. 961–966.

[64] F. Liu, W. Lei, T. Wang, C. Nie, and Y. Wang, "A phase-shift soft-switching control strategy for dual active wireless power transfer system," in *Proc. IEEE Energy Convers. Congr. Expo. (ECCE)*, Cincinnati, OH, USA, Oct. 2017, pp. 2573–2578.

[65] J. R. Sibué, G. Kwimang, J.-P. Ferrieux, G. Meunier, J. Roudet, and R. Périot, "A global study of a contactless energy transfer system: Analytical design, virtual prototyping, and experimental validation," *IEEE Trans. Power Electron.*, vol. 28, no. 10, pp. 4690–4699, Oct. 2013.

[66] J. Jiang, K. Song, Z. Li, C. Zhu, and Q. Zhang, "System modeling and switching control strategy of wireless power transfer system," *IEEE J. Emerg. Sel. Topics Power Electron.*, vol. 6, no. 3, pp. 1295–1305, Sep. 2018.

[67] H. L. Li, A. P. Hu, and G. A. Covic, "A power flow control method on primary side for a CPT system," in *Proc. Int. Power Electron. Conf.-ECCE ASIA*, Sapporo, Japan, Jun. 2010, pp. 1050–1055.

[68] W. Zhang, S.-C. Wong, C. K. Tse, and Q. Chen, "Design for efficiency optimization and voltage controllability of series-series compensated inductive power transfer systems," *IEEE Trans. Power Electron.*, vol. 29, no. 1, pp. 191–200, Jan. 2014.

[69] L. Tan, Z. Zhang, Z. Zhang, B. Deng, M. Zhang, J. Li, and X. Huang, "A segmented power-efficiency coordinated control strategy for bidirectional wireless power transmission systems with variable structural parameters," *IEEE Access*, vol. 6, pp. 40289–40301, 2018.

[70] M. Sasaki and M. Yamamoto, "Exciting voltage control for transfer efficiency maximization for multiple wireless power transfer systems," in *Proc. IEEE Energy Convers. Congr. Expo. (ECCE)*, Cincinnati, OH, USA, Oct. 2017, pp. 5523–5528.

[71] T. Beh, M. Kato, T. Imura, and Y. Hori, "Wireless power transfer system via magnetic resonant coupling at fixed resonance frequency-power transfer system based on impedance matching," *World Electr. Vehicle J.*, vol. 4, no. 4, pp. 744–753, 2010.

[72] H. Li, K. Wang, J. Fang, and Y. Tang, "Pulse density modulated ZVS full-bridge converters for wireless power transfer systems," *IEEE Trans. Power Electron.*, vol. 34, no. 1, pp. 369–377, Jan. 2019.

[73] X. Liu, T. Wang, X. Yang, and H. Tang, "Analysis of efficiency improvement in wireless power transfer system," *IET Power Electron.*, vol. 11, no. 2, pp. 302–309, Feb. 2018.

[74] H. Ishihara, F. Moritsuka, H. Kudo, S. Obayashi, T. Itakura, A. Matsushita, H. Mochikawa, and S. Otaka, "A voltage ratio-based efficiency control method for 3 kW wireless power transmission," in *Proc. IEEE Appl. Power Electron. Conf. Expo. (APEC)*, Fort Worth, TX, USA, Mar. 2014, pp. 1312–1316.

[75] G. Vandevoorde and R. Puers, "Wireless energy transfer for stand-alone systems: A comparison between low and high power applicability," *Sens. Actuators A, Phys.*, vol. 92, nos. 1–3, pp. 305–311, 2000.

[76] R. Bosshard, U. Badstübner, J. W. Kolar, and I. Stevanović, "Comparative evaluation of control methods for inductive power transfer," in *Proc. Int. Conf. Renew. Energy Res. Appl. (ICRERA)*, Nagasaki, Japan, Nov. 2012, pp. 1–6.

[77] J.-I. Itoh, K. Noguchi, and K. Orikawa, "System design of electric assisted bicycle using EDLCs and wireless charger," in *Proc. Int. Power Electron. Conf. (IPEC-Hiroshima-ECCE ASIA)*, Hiroshima, Japan, May 2014, pp. 2277–2284.

[78] C. Zhu, C. Yu, K. Liu, and R. Ma, "Research on the topology of wireless energy transfer device," in *Proc. IEEE Vehicle Power Propuls. Conf. (VPPC)*, Sep. 2008, pp. 1–5.

[79] M. G. Egan, D. L. O'Sullivan, J. G. Hayes, M. J. Willers, and C. P. Henze, "Power-factor-corrected single-stage inductive charger for electric vehicle batteries," *IEEE Trans. Ind. Electron.*, vol. 54, no. 2, pp. 1217–1226, Apr. 2007.

[80] Z. Ouyang, G. Sen, O. C. Thomsen, and M. A. E. Andersen, "Analysis and design of fully integrated planar magnetics for primary–parallel isolated boost converter," *IEEE Trans. Ind. Electron.*, vol. 60, no. 2, pp. 494–508, Feb. 2013.

[81] V. Shevchenko, O. Husev, B. Pakhaliuk, and I. Kondratenko, "Design and simulation verification of low power wireless charging battery system for electric bicycle," in *Proc. IEEE 3rd Int. Conf. Intell. Energy Power Syst. (IEPS)*, Kharkiv, Ukraine, Sep. 2018, pp. 22–27.

[82] S. Nutwong, A. Sangswang, and S. Naetiladdanon, "Output voltage control of the SP topology IPT system using a primary side controller," in *Proc. 13th Int. Conf. Electr. Eng./Electron., Comput., Telecommun. Inf. Technol. (ECTI-CON)*, Chiang Mai, Thailand, Jun./Jul. 2016, pp. 1–5.

[83] B. Ni, C. Y. Chung, and H. L. Chan, "Design and comparison of parallel and series resonant topology in wireless power transfer," in *Proc. IEEE 8th Conf. Ind. Electron. Appl. (ICIEA)*, Jun. 2013, pp. 1832–1837.

[84] W. Zhang, S.-C. Wong, C. K. Tse, and Q. Chen, "Analysis and comparison of secondary series- and parallel-compensated inductive power transfer systems operating for optimal efficiency and load-independent voltage-transfer ratio," *IEEE Trans. Power Electron.*, vol. 29, no. 6, pp. 2979–2990, Jun. 2014.

[85] Z. Huang, S. C. Wong, and C. K. Tse, "Design of a single-stage inductive-power-transfer converter for efficient EV battery charging," *IEEE Trans. Veh. Technol.*, vol. 66, no. 7, pp. 5808–5821, Jul. 2017.

[86] J. Hou, Q. Chen, K. Yan, X. Ren, S.-C. Wong, and C. K. Tse, "Analysis and control of S/SP compensation contactless resonant converter with constant voltage gain," in *Proc. IEEE Energy Convers. Congr. Expo. (ECCE)*, Sep. 2013, pp. 2552–2558.

[87] W. Zhang, S.-C. Wong, C. K. Tse, and Q. Chen, "Load-independent duality of current and voltage outputs of a series-or parallel-compensated inductive power transfer converter with optimized efficiency," *IEEE J. Emerg. Sel. Topics Power Electron.*, vol. 3, no. 1, pp. 137–146, Mar. 2015.

[88] C. Chen, H. Zhou, Q. Deng, W. Hu, Y. Yu, X. Lu, and J. Lai, "Modeling and decoupled control of inductive power transfer to implement constant current/voltage charging and ZVS operating for electric vehicles," *IEEE Access*, vol. 6, pp. 59917–59928, 2018.

[89] C. Wang, R. Lu, C. Zhu, G. Wei, and K. Song, "Characteristics comparison of typical secondary-side compensation topologies in wireless powering systems with constant-current primary-side," in *Proc. IEEE Transp. Electrific. Conf. Expo, Asia–Pacific (ITEC Asia–Pacific)*, Harbin, China, Aug. 2017, pp. 1–6.

[90] N. Jamal, S. Saat, and A. Z. Shukor, "A study on performances of different compensation topologies for loosely coupled inductive power transfer system," in *Proc. IEEE Int. Conf. Control Syst., Comput. Eng.*, Mindeb, Malaysia, Nov./Dec. 2013, pp. 173–178.

[91] N. Jamal, S. Saat, Y. Yusmarnita, T. Zaid, and A. Isa, "Investigations on capacitor compensation topologies effects of different inductive coupling links configurations," *Int. J. Power Electron. Drive Syst.*, vol. 6, no. 2, pp. 274–281, Jun. 2015.

[92] K. Aditya and S. S. Williamson, "Comparative study of series-series and series-parallel topology for long track EV charging application," in *Proc. IEEE Transp. Electrific. Conf. Expo (ITEC)*, Dearborn, MI, USA, Jun. 2014, pp. 1–5.

[93] J. Li, J. Kang, C. Tian, D. Tian, and T. Xie, "Study on wireless power transfer technology with series-series type of magnetic coupling resonance model," in *Proc. 2nd Int. Conf. Comput. Eng., Inf. Sci. Internet Technol. (CII)*, 2017, pp. 225–232.

[94] Z. Qiang, W. Anna, and W. Hao, "Structure analysis of magnetic coupling resonant for wireless power transmission system," in *Proc. AASRI Int. Conf. Ind. Electron. Appl. (IEA)*, 2015, pp. 380–384.

[95] C.-S. Wang, G. A. Covic, and O. H. Stielau, "General stability criterions for zero phase angle controlled loosely coupled inductive power transfer systems," in *Proc. IEEE IECON*, vol. 2, Nov./Dec. 2001, pp. 1049–1054.

[96] B. Esteban, M. Sid-Ahmed, and N. C. Kar, "A comparative study of power supply architectures in wireless EV charging systems," *IEEE Trans. Power Electron.*, vol. 30, no. 11, pp. 6408–6422, Nov. 2015.

[97] T. Diekhans and R. W. D. Doncker, "A dual-side controlled inductive power transfer system optimized for large coupling factor variations and partial load," *IEEE Trans. Power Electron.*, vol. 30, no. 11, pp. 6320–6328, Nov. 2015.

[98] Y. Chen, Z. Kou, Y. Zhang, Z. He, R. Mai, and G. Cao, "Hybrid topology with configurable charge current and charge voltage output-based WPT charger for massive electric bicycles," *IEEE J. Emerg. Sel. Topics Power Electron.*, vol. 6, no. 3, pp. 1581–1594, Sep. 2018.

[99] R. Mai, Y. Chen, Y. Li, Y. Zhang, G. Cao, and Z. He, "Inductive power transfer for massive electric bicycles charging based on hybrid topology switching with a single inverter," *IEEE Trans. Power Electron.*, vol. 32, no. 8, pp. 5897–5906, Aug. 2017.

[100] S. Li, W. Li, J. Deng, T. D. Nguyen, and C. C. Mi, "A double-sided LCC compensation network and its tuning method for wireless power transfer," *IEEE Trans. Veh. Technol.*, vol. 64, no. 6, pp. 2261–2273, Jun. 2015.

[101] W. Li, H. Zhao, S. Li, J. Deng, T. Kan, and C. C. Mi, "Integrated LCC compensation topology for wireless charger in electric and plug-in electric vehicles," *IEEE Trans. Ind. Electron.*, vol. 62, no. 7, pp. 4215–4225, Jul. 2015.

[102] W. Shi, J. Deng, Z. Wang, and X. Cheng, "The start-up dynamic analysis and one cycle control-PD control combined strategy for primary-side controlled wireless power transfer system," *IEEE Access*, vol. 6, pp. 14439–14450, 2018.

[103] Y. Li, Q. Xu, T. Lin, J. Hu, Z. He, and R. Mai, "Analysis and design of load-independent output current or output voltage of a three-coil wireless power transfer system," *IEEE Trans. Transport. Electrific.*, vol. 4, no. 2, pp. 364–375, Jun. 2018.

[104] N. Hatchavanich, M. Konghirun, and A. Saengswang, "LCL—LCCL voltage source inverter with phase shift control for wireless EV charger," in *Proc. IEEE 12th Int. Conf. Power Electron. Drive Syst. (PEDS)*, Honolulu, HI, USA, Dec. 2017, pp. 297–301.

[105] H. Zhao, W. Shu, D. Li, and S. Li, "A novel wireless power charging system for electric bike application," in *Proc. IEEE PELS Workshop Emerg. Technol., Wireless Power (WoW)*, Daejeon, South Korea, Jun. 2015, pp. 1–5.

[106] W. Li, H. Zhao, J. Deng, S. Li, and C. C. Mi, "Comparison study on SS and double-sided LCC compensation topologies for EV/PHEV wireless chargers," *IEEE Trans. Veh. Technol.*, vol. 65, no. 6, pp. 4429–4439, Jun. 2016.

[107] D. Fu, B. Lu, and F. C. Lee, "1 MHz high efficiency LLC resonant converters with synchronous rectifier," in *Proc. IEEE Power Electron. Spec. Conf.*, Orlando, FL, USA, Jun. 2007, pp. 2404–2410.

[108] C. L. Chia and E. K. K. Sng, "A novel robust control method for the series–parallel resonant converter," *IEEE Trans. Power Electron.*, vol. 24, no. 8, pp. 1896–1904, Aug. 2009.

[109] B. Li, G. Zhu, J. Lu, W. Li, G. R. Kumar, and J. Wang, "Output characteristics of LCC-S compensation network and its optimal parameters design in IPT system," *J. Eng.*, vol. 2017, no. 13, pp. 1576–1579, 2017.

[110] X. Meng, D. Qiu, M. Lin, S. C. Tang, and B. Zhang, "Output voltage identification based on transmitting side information for implantable wireless power transfer system," *IEEE Access*, vol. 7, pp. 2938–2946, 2018.

[111] I. Nam, R. Dougal, and E. Santi, "Novel control approach to achieving efficient wireless battery charging for portable electronic devices," in *Proc. IEEE Energy Convers. Congr. Expo. (ECCE)*, Raleigh, NC, USA, Sep. 2012, pp. 2482–2491.

[112] Y. Yao, X. Liu, Y. Wang, and D. Xu, "LC/CL compensation topology and efficiency-based optimisation method for wireless power transfer," *IET Power Electron.*, vol. 11, no. 6, pp. 1029–1037, May 2018.

[113] M. M. Alam, S. Mekhilef, H. Bassi, and M. J. H. Rawa, "Analysis of LC-LC^2 compensated inductive power transfer for high efficiency and load independent voltage gain," *Energies*, vol. 11, no. 11, pp. 2883–2896, 2018.

[114] Z. Dai, J. Wang, M. Long, and H. Huang, "A witricity-based high-power device for wireless charging of electric vehicles," *Energies*, vol. 10, no. 3, p. 323, 2017.

[115] Y. Wang, Y. Yao, X. Liu, D. Xu, and L. Cai, "An LC/S compensation topology and coil design technique for wireless power transfer," *IEEE Trans. Power Electron.*, vol. 33, no. 3, pp. 2007–2025, Mar. 2018.

[116] S. Samanta and A. K. Rathore, "Analysis and design of current-fed (L)(C) (LC) converter for inductive wireless power transfer (IWPT)," in *Proc. IEEE Energy Convers. Congr. Expo. (ECCE)*, Montreal, QC, Canada, Sep. 2015, pp. 5724–5731.

[117] J. Hou, Q. Chen, X. Ren, X. Ruan, S.-C. Wong, and C. K. Tse, "Precise characteristics analysis of series/series-parallel compensated contactless resonant converter," *IEEE J. Emerg. Sel. Topics Power Electron.*, vol. 3, no. 1, pp. 101–110, Mar. 2015.

[118] M. K. Uddin, S. Mekhilef, and G. Ramasamy, "Compact wireless IPT system using a modified voltage-fed multi-resonant class EF2 inverter," *J. Power Electron.*, vol. 18, no. 1, pp. 277–288, 2018.

[119] C. Zhao, Z. Wang, J. Du, J. Wu, S. Zong, and X. He, "Active resonance wireless power transfer system using phase shift control strategy," in *Proc. IEEE Appl. Power Electron. Conf. Expo. (APEC)*, Fort Worth, TX, USA, Mar. 2014, pp. 1336–1341.

[120] S. Nutwong, A. Sangswang, and S. Naetiladdanon, "Design of the wireless power transfer system with uncompensated secondary to increase power transfer capability," in *Proc. 8th IET Int. Conf. Power Electron., Mach. Drives*, Apr. 2016, pp. 1–5.

[121] V.-B. Vu, V.-T. Phan, M. Dahidah, and V. Pickert, "Multiple output inductive charger for electric vehicles," *IEEE Trans. Power Electron.*, vol. 34, no. 8, pp. 7350–7368, Aug. 2018.

[122] C. Jiang, K. T. Chau, C. Liu, and C. H. T. Lee, "An overview of resonant circuits for wireless power transfer," *Energies*, vol. 10, no. 7, p. 894, 2017.

[123] S. Y. R. Hui, W. Zhong, and C. K. Lee, "A critical review of recent progress in mid-range wireless power transfer," *IEEE Trans. Power Electron.*, vol. 29, no. 9, pp. 4500–4511, Sep. 2014.

[124] J. Zhang, X. Yuan, C. Wang, and Y. He, "Comparative analysis of two-coil and three-coil structures for wireless power transfer," *IEEE Trans. Power Electron.*, vol. 32, no. 1, pp. 341–352, Jan. 2017.

[125] T. Arakawa, S. Goguri, J. V. Krogmeier, A. Kruger, D. J. Love, R. Mudumbai, and M. A. Swabey, "Optimizing wireless power transfer from multiple transmit coils," *IEEE Access*, vol. 6, pp. 23828–23838, 2018.

[126] B. Pakhaliuk, O. Husev, V. Shevchenko, O. Veligorskyi, and K. Kroics, "Novel inductive power transfer approach based on Z-source network with compensation circuit," in *Proc. IEEE 38th Int. Conf. Electron. Nanotechnol. (ELNANO)*, Kiev, Ukraine, Apr. 2018, pp. 699–704.

[127] C. Xia, Y. Liu, K. Lin, and G. Xie, "Model and frequency control for three-phase wireless power transfer system," *Math. Problems Eng.*, vol. 2016, Sep. 2016, Art. no. 3853146.

[128] M. R. A. Khandaker, K.-K. Wong, Y. Zhang, and Z. Zheng, "Probabilistically robust SWIPT for secrecy MISOME systems," *IEEE Trans. Inf. Forensics Security*, vol. 12, no. 1, pp. 211–226, Jan. 2017.

[129] S. Y. R. Hui and W. W. C. Ho, "A new generation of universal contactless battery charging platform for portable consumer electronic equipment," *IEEE Trans. Power Electron.*, vol. 20, no. 3, pp. 620–627, May 2005.

[130] B.-M. Song, R. Kratz, and S. Gurol, "Contactless inductive power pickup system for Maglev applications," in *Proc. Conf. Rec. IEEE IAS Annu. Meeting*, vol. 3, Oct. 2002, pp. 1586–1591.

[131] U. K. Madawala and D. J. Thrimawithana, "A bidirectional inductive power interface for electric vehicles in V2G systems," *IEEE Trans. Ind. Electron.*, vol. 58, no. 10, pp. 4789–4796, Oct. 2011.

[132] J. Kuang, B. Luo, Y. Zhang, Y. Hu, and Y. Wu, "Load-isolation wireless power transfer with K-inverter for multiple-receiver applications," *IEEE Access*, vol. 6, pp. 31996–32004, 2018.

[133] H. Nguyen, J. I. Agbinya, and J. Devlin, "Channel characterisation and link budget of MIMO configuration in near field magnetic communication," *Int. J. Electron. Telecommun.*, vol. 59, no. 3, pp. 255–262, Aug. 2013.

[134] H. Han, Z. Mao, Q. Zhu, M. Su, and A. P. Hu, "A 3D wireless charging cylinder with stable rotating magnetic field for multi-load application," *IEEE Access*, vol. 7, pp. 35981–35997, 2019.

[135] H. Hao, G. A. Covic, and J. T. Boys, "A parallel topology for inductive power transfer power supplies," *IEEE Trans. Power Electron.*, vol. 29, no. 3, pp. 1140–1151, May 2014.

[136] L. Shi, Z. Yin, L. Jiang, and Y. Li, "Advances in inductively coupled power transfer technology for rail transit," *CES Trans. Elect. Mach. Syst.*, vol. 1, no. 4, pp. 383–396, Dec. 2017.

[137] K. A. Kalwar, M. Aamir, and S. Mekhilef, "A design method for developing a high misalignment tolerant wireless charging system for electric vehicles," *Measurement*, vol. 118, pp. 237–245, Mar. 2018.

[138] X. Qu, H. Han, S.-C. Wong, C. K. Tse, and W. Chen, "Hybrid IPT topologies with constant current or constant voltage output for battery charging applications," *IEEE Trans. Power Electron.*, vol. 30, no. 11, pp. 6329–6337, Nov. 2015.

[139] R. Bosshard, J. W. Kolar, and B. Wunsch, "Control method for inductive power transfer with high partial-load efficiency and resonance tracking," in *Proc. Int. Power Electron. Conf. (IPEC-Hiroshima-ECCE ASIA)*, Hiroshima, Japan, May 2014, pp. 2167–2174.

[140] C. Li, X. Zhao, C. Liao, and L. Wang, "A graphical analysis on compensation designs of large-gap CPT systems for EV charging applications," *CES Trans. Elect. Mach. Syst.*, vol. 2, no. 2, pp. 232–242, Jun. 2018.

[141] G. A. Covic, G. Elliott, O. H. Stielau, R. M. Green, and J. T. Boys, "The design of a contact-less energy transfer system for a people mover system," in *Proc. Int. Conf. Power Syst. Technol.*, vol. 1, Dec. 2000, pp. 79–84.

[142] J. Yuan, F. Xiao, C. Zhang, Z. Ni, and Y. Zhong, "A hybrid negative current compensation system for high-speed railway power system," in *Proc. IEEE Appl. Power Electron. Conf. Expo. (APEC)*, San Antonio, TX, USA, Mar. 2018, pp. 1461–1466.

[143] M. Petersen and F. W. Fuchs, "Investigation on power electronics topologies for inductive power transfer (IPT) systems in high power low voltage applications," in *Proc. 17th Eur. Conf. Power Electron. Appl. (EPE ECCE-Eur.)*, Geneva, Switzerland, Sep. 2015, pp. 1–10.

[144] Y. Yang, Y. Benomar, M. El Baghdadi, O. Hegazy, and J. Van Mierlo, "Design, modeling and control of a bidirectional wireless power transfer for light-duty vehicles: G2V and V2G systems," in *Proc. 19th Eur. Conf. Power Electron. Appl. (EPE ECCE Eur.)*, Warsaw, Poland, Sep. 2017, pp. P.1–P.12.

[145] K. A. Kalwar, M. Aamir, and S. Mekhilef, "Inductively coupled power transfer (ICPT) for electric vehicle charging—A review," *Renew. Sustain. Energy Rev.*, vol. 47, pp. 462–475, Jul. 2015.

[146] C. Auvigne, P. Germano, D. Ladas, and Y. Perriard, "A dual-topology ICPT applied to an electric vehicle battery charger," in *Proc. Int. Conf. Elect. Mach.*, Sep. 2012, pp. 2287–2292.

[147] H. Z. Z. Beh, G. A. Covic, and J. T. Boys, "Wireless fleet charging system for electric bicycles," *IEEE J. Emerg. Sel. Topics Power Electron.*, vol. 3, no. 1, pp. 75–86, Mar. 2015.

[148] A. Okuno, L. Gamage, and M. Nakaoka, "Performance evaluations of high-frequency inverter-linked DC/DC converter with noncontact pickup coil," *IEEE Trans. Ind. Electron.*, vol. 48, no. 2, pp. 475–477, Apr. 2001.

[149] A. Esser and H.-C. Skudelny, "A new approach to power supplies for robots," *IEEE Trans. Ind. Appl.*, vol. 27, no. 5, pp. 872–875, Sep. 1991.

[150] B. J. Heeres, D. W. Novotny, D. M. Divan, and R. D. Lorenz, "Contactless underwater power delivery," in *Proc. Power Electron. Spec. Conf. (PESC)*, vol. 1, Jun. 1994, pp. 418–423.

[151] W. Niu, W. Gu, and J. Chu, "Analysis and experimental results of frequency splitting of underwater wireless power transfer," *J. Eng.*, vol. 2017, no. 7, pp. 385–390, Jul. 2017.

[152] W. Zhong, C. K. Lee, and S. Y. R. Hui, "General analysis on the use of Tesla's resonators in domino forms for wireless power transfer," *IEEE Trans. Ind. Electron.*, vol. 60, no. 1, pp. 261–270, Jan. 2013.

[153] Y. Lu and D. B. Ma, "Wireless power transfer system architectures for portable or implantable applications," *Energies*, vol. 9, no. 12, p. 1087, 2016.

[154] H.-J. Kim, H. Hirayama, S. Kim, K. J. Han, R. Zhang, and J.-W. Choi, "Review of near-field wireless power and communication for biomedical applications," *IEEE Access*, vol. 5, pp. 21264–21285, 2017.

[155] Q. Chen, S. C. Wong, C. K. Tse, and X. Ruan, "Analysis, design, and control of a transcutaneous power regulator for artificial hearts," *IEEE Trans. Biomed. Circuits Syst.*, vol. 3, no. 1, pp. 23–31, Feb. 2009.

[156] Y. Jang and M. M. Jovanovic, "A contactless electrical energy transmission system for portable-telephone battery chargers," *IEEE Trans. Ind. Electron.*, vol. 50, no. 3, pp. 520–527, Jun. 2003.

[157] Y. Jang and M. M. Jovanovic, "A contactless electrical energy transmission system for portable-telephone battery chargers," in *Proc. 22nd Conf. Rec. Telecommun. Energy Conf.*, Sep. 2000, pp. 726–732.

[158] *Wireless Power Transfer and Charging*. [Online]. Available: http://www.designhmi.com/2015/04/16/wireless-power-transfer-and-charging/

[159] Z. Yan, Q. Siyao, Q. Zhu, L. Huang, and A. P. Hu, "A simple brightness and color control method for LED lighting based on wireless power transfer," *IEEE Access*, vol. 6, pp. 51477–51483, 2018.

[160] M. Su, Z. Liu, Q. Zhu, and A. P. Hu, "Study of maximum power delivery to movable device in omnidirectional wireless power transfer system," *IEEE Access*, vol. 6, pp. 76153–76164, 2018.

[161] K. Throngnumchai, A. Hanamura, Y. Naruse, and K. Takeda, "Design and evaluation of a wireless power transfer system with road embedded transmitter coils for dynamic charging of electric vehicles," in *Proc. World Electr. Vehicle Symp. Exhib. (EVS)*, Barcelona, Spain, 2013, pp. 1–10.

VIKTOR SHEVCHENKO (S'18) was born in Ukraine, in 1990. He received the B.Sc. and M.Sc. degrees in industrial electronics from the Chernihiv National University of Technology, Chernihiv, Ukraine, in 2015 and 2017, respectively. He is currently pursuing the Ph.D. degree in 2017.

He is currently a Junior Researcher and a Teacher's Assistant with the Department of Biomedical Radioelectronics Apparatus and Systems, Chernihiv National University of Technology. He has several publications and patents. His current research interests include power electronics systems, wireless power transfer, and photovoltaic systems.

OLEKSANDR HUSEV (S'10–M'12–SM'19) received the B.Sc. and M.Sc. degrees in industrial electronics from Chernihiv State Technological University, Chernihiv, Ukraine, in 2007 and 2008, respectively. He defended the Ph.D. thesis from the Institute of Electrodynamics, National Academy of Science of Ukraine, in 2012.

He is currently a Senior Researcher with the Department of Electrical Power Engineering and Mechatronics, Tallinn University of Technology, and also an Associate Professor with the Department of Biomedical Radioelectronics Apparatus and Systems, Chernihiv National University of Technology. He has more than 100 publications and is the holder of several patents. His research interests include power electronics systems, the design of novel topologies, control systems based on a wide range of algorithms, including modeling, design, and simulation, the applied design of power converters and control systems and application, and stability investigation.

RYSZARD STRZELECKI graduated in electronics and automation from the Kyiv University of Technology, in 1981, and received the Ph.D. degree in 1984, and the Habilitation (D.Sc.) degree in prediction control of the self-commutation power electronics converters from the Institute of Electrodynamics, Academy of Sciences, Ukrainian Soviet Republic, Kiev, in 1991. In 1999, he received the title of Professor of Technical Sciences. He is currently a Full Professor with the Faculty of Electrical and Control Engineering, Gdansk University of Technology, and with ITMO University, the Head of the Baltic Laboratory of Power Electronics Technology, Gdynia, and also the Head of the Electrical Engineering Institute, Warsaw. He has authored more than 200 journals and conferences articles, six monographs, and holds 13 patents. His research interests include topologies and control methods and the industrial application of power electronic systems, in particular to improve power quality, and power flow control.

BOHDAN PAKHALIUK (S'18) received the B.Sc. and M.Sc. degrees in industrial electronics from the Chernihiv National University of Technology, Chernihiv, Ukraine, in 2016 and 2018, respectively. He is currently pursuing the Ph.D. degrees with the Gdansk University of Technology and also with the Chernihiv National University of Technology. He is currently a Junior Researcher with the Department of Biomedical Radioelectronics Apparatus and Systems, Chernihiv National University of Technology. His research interests include design and control converters for wireless power transfer applications.

NIKOLAI POLIAKOV received the B.S. and M.S. degrees in electrical engineering from ITMO University, Saint Petersburg, Russia, in 2009 and 2011, respectively. He defended the Ph.D. thesis from ITMO University, Russia, in 2016.

He is currently an Associate Professor with the Faculty of Control Engineering and Robotics, ITMO University. His current research interests include power converters design, power electronics, power efficiency, wireless power transfer systems, and control theory and its applications.

NATALIA STRZELECKA graduated in electronics and automation from the Kyiv University of Technology, in 1981. In 2014, she defended the Ph.D. thesis from Gdynia Maritime University, Poland.

She is currently an Assistant Professor with the Faculty of Electrical Engineering, Gdynia Maritime University. Her current research interests include the analytical and computer modeling of the power electronics systems.

• • •